

This Page Is Inserted by IFW Operations  
and is not a part of the Official Record

## **BEST AVAILABLE IMAGES**

Defective images within this document are accurate representations of the original documents submitted by the applicant.

Defects in the images may include (but are not limited to):

- BLACK BORDERS
- TEXT CUT OFF AT TOP, BOTTOM OR SIDES
- FADED TEXT
- ILLEGIBLE TEXT
- SKEWED/SLANTED IMAGES
- COLORED PHOTOS
- BLACK OR VERY BLACK AND WHITE DARK PHOTOS
- GRAY SCALE DOCUMENTS

**IMAGES ARE BEST AVAILABLE COPY.**

**As rescanning documents *will not* correct images,  
please do not report the images to the  
Image Problem Mailbox.**

secondary structure defined by:

- five nucleotides forming a first side of a first double stranded region;  
four nucleotides forming a first side of a first end loop region;  
five nucleotides forming a second side of said first double stranded region;  
two nucleotides forming a bulge between said first double stranded region and a second double stranded region;  
five nucleotides forming a first side of said second double stranded region;  
three nucleotides forming a second end loop region; and  
five nucleotides forming a second side of said second double stranded region.

102  
E cont'd

95. (Amended) The RNA of claim 94 wherein said nucleotides forming said first side of said first double stranded region are of the sequence NNNGA, UAAGA, AAAGA, UAUGA, or UUUGA and said nucleotides forming said second side of said first double stranded region are of the sequence UUNNG, UUUUG, or UUCUG.

103  
E

108. (Amended twice) A purified and isolated RNA comprising the consensus sequence NNNGAUNCUUUNNGUAAGCCCNANGNGNN (SEQ ID NO:23) and having a first double stranded region, a first end loop region, a second double stranded region, and a second end loop region.

### REMARKS

Claims 87-100, 108, and 110-113 are pending in the present application. Claims 1-86, 101-107 and 109, drawn to non-elected inventions, have been cancelled without prejudice to their presentation in another application. Claims 87, 88, 94, 95, and 108 have been amended herein. Upon entry of the present amendment, claims 87-100, 108, and 110-113 will remain pending.

As a preliminary matter, Applicants have deleted Figures 55, 56, 58-63, 65-125, 128-138, and 145, which are not required to comply with the requirements of 35 U.S.C. § 112 in regard to the claimed invention. Originally filed drawing Figures 57, 64, 126, 127, 139-144, and 146-158 have

been renumbered as Figures 55-77, respectively.

Furthermore, in response to the Draftsperson's objections, originally filed drawing Figures 41 and 42 have each been divided into two figures and renumbered as Figures 41A, 41B, 42A, and 42B, respectively. The separation was necessary to allow enlargement of the mass spectrums for enhanced clarity. No new matter has been added to the drawings.

Formal drawings of all of the non-cancelled Figures have been filed on date herewith under separate cover to the Draftsperson. Figures objected to by the Draftsperson have been corrected.

In addition, Applicants have amended the specification, as requested by the Examiner, to delete hyperlinks and other forms of browser-executable code. Applicants have also amended the specification to correct typographical errors and to delete a section at page 72, line 28 through page 89, line 7 that was inadvertently duplicated.

Applicants have amended claims 87 and 108 as recommended by the Examiner to overcome the 35 U.S.C. § 101 rejection. In particular, claims 87 and 94 have been amended to address the concern in the Office Action that there was indefinite antecedent bases for the phrase "second double stranded region." In addition, Applicants have amended claims 88 and 95 to correct typographical errors in the sequence listings. Originally filed Figure 127 (changed to Figure 56 by this amendment) clearly show that the original sequence listings in claims 88 and 95 were typographical errors. No new matter has been added.

New pages 1-41 are provided to comply with the Sequence Rules set forth in 37 C.F.R. §§ 1.821-1.825. Enclosed herewith is a Statement to Support Filing and Submission of DNA/Amino Acid Sequences in Accordance with 37 C.F.R. §§ 1.821 through 1.825 and a computer readable form (CRF). No new matter has been added. In addition, the contents of the paper copy of the Sequence Listing and computer readable copy of the Sequence Listing, submitted in accordance with 37 C.F.R. § 1.821(c) and (e), are the same.

**I. The Claimed Invention Is Novel****A. The McKnight Reference**

Claims 87-100, 108, 110, 112, and 113 stand rejected under 35 U.S.C. § 102(b) as allegedly being anticipated by McKnight *et al.*, *Immunogenetics.*, **1989**, 30, 145-47 (hereinafter, the “McKnight reference”). Applicants traverse the rejection and respectfully request reconsideration thereof because the McKnight reference fails to teach every element recited in the claims.

The McKnight reference reports a cDNA sequence of a rat IL-2 clone that contains a 5’ untranslated region, coding region, and 3’ untranslated region in Figure 1. In total, the reported cDNA sequence contains 740 nucleotides. The McKnight reference fails to teach any secondary structure associated with the 740 nucleotide cDNA sequence.

The Office Action incorrectly asserts that the McKnight reference teaches an RNA comprising SEQ ID NO:23 and SEQ ID NO:25 and having at least twenty-nine but no more than seventy nucleotides, which contains the secondary structure recited in claim 87. Regardless of whether the cDNA sequence reported in the McKnight reference comprises the secondary structure recited in claim 87 (and Applicants submit that the Office Action utterly fails to establish that such secondary structure is inherent in the reported cDNA sequence), the McKnight reference fails to teach an RNA comprising “not more than seventy nucleotides.” A prior art reference anticipates a claim if every element of the claim appears in the prior art reference. *Glaxo Inc. v. Novopharm, Ltd.*, 52 F.3d 1043, 1047, 34 U.S.P.Q.2d 1565, 1567 (Fed. Cir. 1995). Because the cDNA sequence reported in the McKnight reference is 740 nucleotides in length, it does not anticipate claim 87 (nor dependent claims 88-93), which recites an RNA “not more than seventy nucleotides.”

Claims 94-100 and 108 recite an RNA having a particular secondary structure. It is undisputed that the McKnight reference fails to disclose any secondary structure of the 740 nucleotide cDNA sequence reported therein. Nonetheless, the Office Action assumes that the McKnight cDNA comprises the secondary structure recited in claims 94-100 and 108. Thus, it appears that the Office Action asserts that the secondary structure recited in Applicants’ claims is inherent in the McKnight cDNA sequence. To anticipate a claim, however, a prior art reference must disclose every feature of the claimed invention, either explicitly or inherently. *Glaxo v. Novopharm*,

*Ltd.*, 334 U.S.P.Q.2d 1565 (Fed. Cir. 1995). Further, to serve as an anticipation when a reference is silent about the alleged inherent characteristic, such gap in the reference may be filled by extrinsic evidence. Such evidence, however, must make clear that the missing descriptive matter is necessarily (*i.e.*, always) present in the thing described in the reference, and that it would be so recognized by persons of ordinary skill in the art. *In re Oelrich*, 40 U.S.P.Q. 323 (C.C.P.A. 1981); *Continental Can Co. USA Inc. v. Monsanto Co.*, 20 U.S.P.Q.2d 1746 (Fed. Cir. 1991). Inherency may not be established by probabilities or possibilities. *Id.* Further, the mere fact that a certain thing may result from a given set of circumstances is not sufficient. *Id.* Significantly, the Office Action has not established that the critical inherent characteristics are necessarily present in the McKnight reference. Indeed, the Office Action fails to provide any extrinsic evidence that makes clear that the missing descriptive matter is always present in the thing described in the McKnight reference, and that it would be so recognized by persons of ordinary skill in the art. Thus, Office Action has failed to establish that the McKnight reference anticipates claims 94-100 and 108.

Claims 110, 112 and 113 recite an “RNA fragment.” In contrast, the McKnight reference reports a cDNA sequence containing the 5’ untranslated region, coding region, and 3’ untranslated region -- *i.e.*, a cDNA containing the entire gene. Aside from the fact that the sequence reported in Figure 1 of the McKnight reference is a cDNA sequence and not a “purified and isolated RNA,” it is also not a “fragment.” A reference that requires picking and choosing among options disclosed in the reference to such a degree that one skilled in the art would not recognize the claimed invention does not anticipate the claimed invention. *See In re Arkley*, 172 U.S.P.Q. 524, 526 (C.C.P.A. 1972); *In re Ruschig*, 145 U.S.P.Q. 274, 282 (C.C.P.A. 1965). In the present case, the McKnight reference does not even present Applicants’ claimed inventions as options. In addition, the Office Action fails to assert, let alone prove, that the McKnight sequence is “conserved across at least two species,” as recited in claim 110. Thus, the McKnight reference also fails to anticipate claims 110, 112, and 113.

In view of the foregoing, the McKnight reference fails to anticipate claims 87-100, 108, 110, 112 and 113. Accordingly, Applicants respectfully request that the rejection under 35 U.S.C. § 102(b) be withdrawn.

**B. The Chen Reference**

Claims 87-100, 108, 110, and 111 stand rejected under 35 U.S.C. § 102(b) as allegedly being anticipated by Chen *et al.*, *Proc. Natl. Acad. Sci. USA*, **1985**, 82, 7284-7288 (hereinafter, the “Chen reference”). Applicants traverse the rejection and respectfully request reconsideration thereof because the Chen reference fails to teach every element recited in the rejected claims.

The Chen reference reports a cDNA sequence of a human IL-2 clone and two gibbon IL-2 clones that contains a 5’ untranslated region, coding region, and 3’ untranslated region in Figure 3. In total, the reported cDNA sequences each contain from about 800 to 1000 nucleotides. The Chen reference fails to teach any secondary structure associated with the cDNA sequences reported therein.

In similar fashion to the rejection over the McKnight reference, the Office Action incorrectly asserts that the Chen reference teaches an RNA comprising SEQ ID NO:24 and having at least twenty-nine but no more than seventy nucleotides, which contains the secondary structure recited in claim 87. Regardless of whether the cDNA sequences reported in the Chen reference comprise the secondary structure recited in claim 87 (and Applicants submit that the Office Action utterly fails to establish that such secondary structure is inherent in the reported cDNA sequences), the Chen reference fails to teach an RNA comprising “not more than seventy nucleotides.” As stated above, a prior art reference anticipates a claim if every element of the claim appears in the prior art reference. Because the cDNA sequences reported in the Chen reference are at least 800 to 1000 nucleotides in length, it does not anticipate claim 87 (nor dependent claims 88-93), which recites an RNA “not more than seventy nucleotides.”

Claims 94-100 and 108 recite an RNA having a particular secondary structure. It is undisputed that the Chen reference fails to disclose any secondary structure of the at least 800 nucleotide cDNA sequences reported therein. Nonetheless, the Office Action assumes that the Chen cDNA comprises the secondary structure recited in claims 94-100 and 108. Thus, it appears that the Office Action asserts that the secondary structure recited in Applicants’ claims is inherent in the Chen cDNA sequence. As stated above, to anticipate a claim, a prior art reference must disclose every feature of the claimed invention, either explicitly or inherently, and any gaps may be filled by

extrinsic evidence. Significantly, the Office Action has not established that the secondary structure recited in the claims is necessarily present in the Chen reference. Indeed, the Office Action fails to provide any extrinsic evidence that makes clear that the missing descriptive matter is always present in the thing described in the Chen reference, and that it would be so recognized by persons of ordinary skill in the art. Thus, Office Action has failed to establish that the Chen reference anticipates claims 94-100 and 108.

Claims 110 and 111 recite an “RNA fragment.” In contrast, the Chen reference reports cDNA sequences containing the 5’ untranslated region, coding region, and 3’ untranslated region -- *i.e.*, cDNAs containing the entire gene. Aside from the fact that the sequence reported in Figure 3 of the Chen reference is a cDNA sequence and not a “purified and isolated RNA,” it is also not a “fragment.” As stated above, a reference that requires picking and choosing among options disclosed in the reference to such a degree that one skilled in the art would not recognize the claimed invention does not anticipate the claimed invention. The Chen reference fails to particularly point out nucleotides 650 to 678. Indeed, Applicants’ specification provides the only basis for selecting a fragment comprising the recited nucleotide sequence. Further, in the present case, the Chen reference does not even present Applicants’ claimed inventions as options. Thus, the Chen reference also fails to anticipate claims 110 and 111.

In view of the foregoing, the Chen reference fails to anticipate claims 87-100, 108, 110, and 111. Accordingly, Applicants respectfully request that the rejection under 35 U.S.C. § 102(b) be withdrawn.

### **C. The Fu Reference**

Claims 87-91, 94-98, 108, 110, 112, and 113 stand rejected under 35 U.S.C. § 102(e) as allegedly being anticipated by U.S. Patent No. 6,090,620 (hereinafter, the “Fu reference”). Applicants traverse the rejection and respectfully request reconsideration thereof because the Fu reference fails to teach every element recited in the rejected claims.

The Examiner asserts that the Fu reference teaches genomic DNA encoding the WRN gene, which encodes RNA comprising SEQ ID NOS:23 and 25, having at least twenty-nine but not more

than seventy nucleotides. The only sequence within the Fu reference that the Examiner specifically identifies is nucleotides 26015 to 26041 within SEQ ID NO:209, which AGTTTCTTTTGGGAAGCACTTAGAGCT and which is only twenty-seven nucleotides in length. SEQ ID NO:209 reported in the Fu reference is 51,259 nucleotides long.

In similar fashion to the rejections over the McKnight and Chen references, the Office Action incorrectly asserts that the Fu reference teaches an RNA comprising SEQ ID NOs:23 and 24, and having at least twenty-nine but no more than seventy nucleotides, which contains the secondary structure recited in claim 87. Regardless of whether the DNA sequence reported in SEQ ID NO:209 of the Fu reference comprises the secondary structure recited in claim 87 (and Applicants submit that the Office Action utterly fails to establish that such secondary structure is inherent in the reported DNA sequence), the Fu reference fails to teach an RNA comprising “not more than seventy nucleotides.” As stated above, a prior art reference anticipates a claim if every element of the claim appears in the prior art reference. Because the DNA sequences reported in the Fu reference contains more than 50,000 nucleotides, it does not anticipate claim 87 (nor dependent claims 88-91), which recites an RNA “not more than seventy nucleotides.” Further, it is not even clear how the cited portion of the genomic DNA sequence reported in SEQ ID NO:209 of the Fu reference encodes RNA comprising SEQ ID NOs:23 and 25.

Claims 94-98 and 108 recite an RNA having a particular secondary structure. It is undisputed that the Fu reference fails to disclose any secondary structure for the 50,000+ nucleotide sequence of SEQ ID NO:209 or the cited portion thereof. Nonetheless, the Office Action assumes that the Fu DNA comprises the secondary structure recited in claims 94-98 and 108. Thus, it appears that the Office Action asserts that the secondary structure recited in Applicants’ claims is inherent in the Fu DNA sequence. As stated above, to anticipate a claim, a prior art reference must disclose every feature of the claimed invention, either explicitly or inherently, and any gaps may be filled by extrinsic evidence. Significantly, the Office Action has not established that the secondary structure recited in the claims is necessarily present in the Fu reference. Indeed, the Office Action fails to provide any extrinsic evidence that makes clear that the missing descriptive matter is always present in the thing described in the Fu reference, and that it would be so recognized by persons of ordinary



skill in the art. Thus, Office Action has failed to establish that the Fu reference anticipates claims 94-98 and 108.

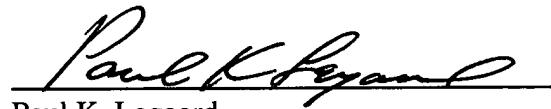
Claims 110, 112 and 113 recite an “RNA fragment.” In contrast, the Fu reference reports a genomic DNA sequence. Aside from the fact that the sequence reported in SEQ ID NO:209 of the Fu reference is genomic DNA and not a “purified and isolated RNA,” it is also not a “fragment.” As stated above, a reference that requires picking and choosing among options disclosed in the reference to such a degree that one skilled in the art would not recognize the claimed invention does not anticipate the claimed invention. Further, in the present case, SEQ ID NO:209 of the Fu reference does not even teach the nucleotide sequences recited in claims 110, 112 and 113. In addition, the Office Action fails to assert, let alone prove, that SEQ ID NO:209 or any portion thereof is “conserved across at least two species,” as recited in claim 110. Thus, the Fu reference also fails to anticipate claims 110, 112 and 113.

In view of the foregoing, the Fu reference fails to anticipate claims 87-91, 94-98, 108, 110, 112, and 113. Accordingly, Applicants respectfully request that the rejection under 35 U.S.C. § 102(e) be withdrawn.

**II. Conclusion**

In view of the foregoing, Applicants respectfully submit that the claims are in condition for allowance. An early notice of the same is earnestly solicited. The Examiner is invited to contact Applicants' undersigned representative at (215) 564-8906 if there are any questions regarding Applicants' claimed invention. Attached hereto is a marked-up version of the changes made to the specification and claims by the current amendment. The attached page is captioned "**Version with markings to show changes made.**"

Respectfully submitted,

A handwritten signature in cursive script, reading "Paul K. Legaard", is written over a horizontal line.

Paul K. Legaard  
Registration No. 38,534

Date: January 30, 2002

WOODCOCK WASHBURN LLP  
One Liberty Place - 46th Floor  
Philadelphia, PA 19103  
Telephone: (215) 568-3100  
Facsimile: (215) 568-3439

**VERSION WITH MARKINGS TO SHOW CHANGES MADE****In the Specification:**

Amend paragraph referring to Figure 41 beginning at page 26, line 1 of the specification as follows:

[Figure 41 shows] Figures 41A and 41B show the ESI-CID-MS of a 27-mer RNA/DNA hybrid in the presence and absence of paromomycin, respectively.

Amend paragraph referring to Figure 42 beginning at page 26, line 3 of the specification as follows:

[Figure 42 shows] Figures 42A and 42B show the ESI-MS of a 27-mer RNA/DNA hybrid target in the presence of paromomycin alone (panel a), and in the presence of both paromomycin and a combinatorial library (panel b), respectively.

Delete paragraph referring to Figure 55 beginning at page 26, line 23 of the specification.

Delete paragraph referring to Figure 56 beginning at page 26, line 25 of the specification.

Amend paragraph referring to Figure 57 beginning at page 26, line 27 of the specification as follows:

Figure 55 [57] shows a representative flow scheme showing preferred steps for a preferred SEALS strategy.

Delete paragraph referring to Figure 58 beginning at page 26, line 29 of the specification.

Delete paragraph referring to Figure 59 beginning at page 27, line 1 of the specification.

Delete paragraph referring to Figure 60 beginning at page 27, line 3 of the specification.

Delete paragraph referring to Figure 61 beginning at page 27, line 5 of the specification.

Delete paragraph referring to Figure 62 beginning at page 27, line 7 of the specification.

Delete paragraph referring to Figure 63 beginning at page 27, line 8 of the specification.

Amend paragraph referring to Figure 64 beginning at page 27, line 9 of the specification as follows:

Figure 56 [64] shows a representative flow scheme showing preferred steps for a preferred Structure Predictor strategy.

Delete paragraph referring to Figure 65 beginning at page 27, line 11 of the specification.  
Delete paragraph referring to Figure 66 beginning at page 27, line 12 of the specification.  
Delete paragraph referring to Figure 67 beginning at page 27, line 13 of the specification.  
Delete paragraph referring to Figure 68 beginning at page 27, line 14 of the specification.  
Delete paragraph referring to Figure 69 beginning at page 27, line 15 of the specification.  
Delete paragraph referring to Figure 70 beginning at page 27, line 17 of the specification.  
Delete paragraph referring to Figure 71 beginning at page 27, line 18 of the specification.  
Delete paragraph referring to Figure 72 beginning at page 27, line 19 of the specification.  
Delete paragraph referring to Figure 73 beginning at page 27, line 20 of the specification.  
Delete paragraph referring to Figure 74 beginning at page 27, line 21 of the specification.  
Delete paragraph referring to Figure 75 beginning at page 27, line 22 of the specification.  
Delete paragraph referring to Figure 76 beginning at page 27, line 23 of the specification.  
Delete paragraph referring to Figure 77 beginning at page 27, line 24 of the specification.  
Delete paragraph referring to Figure 78 beginning at page 27, line 25 of the specification.  
Delete paragraph referring to Figure 79 beginning at page 27, line 26 of the specification.  
Delete paragraph referring to Figure 80 beginning at page 27, line 28 of the specification.  
Delete paragraph referring to Figure 81 beginning at page 27, line 29 of the specification.  
Delete paragraph referring to Figure 82 beginning at page 27, line 30 of the specification.  
Delete pages 28-29 of the specification.

Delete paragraph referring to Figure 114 beginning at page 30, line 1 of the specification.  
Delete paragraph referring to Figure 115 beginning at page 30, line 3 of the specification.  
Delete paragraph referring to Figure 116 beginning at page 30, line 5 of the specification.

Delete paragraph referring to Figure 117 beginning at page 30, line 6 of the specification.  
Delete paragraph referring to Figure 118 beginning at page 30, line 7 of the specification.  
Delete paragraph referring to Figure 119 beginning at page 30, line 8 of the specification.  
Delete paragraph referring to Figure 120 beginning at page 30, line 9 of the specification.  
Delete paragraph referring to Figure 121 beginning at page 30, line 10 of the specification.  
Delete paragraph referring to Figure 122 beginning at page 30, line 11 of the specification.  
Delete paragraph referring to Figure 123 beginning at page 30, line 12 of the specification.  
Delete paragraph referring to Figure 124 beginning at page 30, line 13 of the specification.  
Delete paragraph referring to Figure 125 beginning at page 30, line 14 of the specification.

Amend paragraph referring to Figure 126 beginning at page 30, line 15 of the specification as follows:

Figure 57 [126] shows a representative Dome structure view of region 3 of IL-2 3' UTR. [SEQ ID NO:287, SEQ ID NO:288, SEQ ID NO:289, SEQ ID NO:290, SEQ ID NO:291, SEQ ID NO:292, SEQ ID NO:293, and SEQ ID NO:294] SEQ ID NO:44, SEQ ID NO:45, SEQ ID NO:46, SEQ ID NO:47, SEQ ID NO:48, SEQ ID NO:49, SEQ ID NO:50, and SEQ ID NO:51 are shown top to bottom, respectively.

Amend paragraph referring to Figure 127 beginning at page 30, line 16 of the specification as follows:

Figure 58 [127] shows a representative structure drawing of region 3 of IL-2 3' UTR.

Delete paragraph referring to Figure 128 beginning at page 30, line 17 of the specification.  
Delete paragraph referring to Figure 129 beginning at page 30, line 18 of the specification.  
Delete paragraph referring to Figure 130 beginning at page 30, line 19 of the specification.  
Delete paragraph referring to Figure 131 beginning at page 30, line 20 of the specification.  
Delete paragraph referring to Figure 132 beginning at page 30, line 21 of the specification.  
Delete paragraph referring to Figure 133 beginning at page 30, line 22 of the specification.

Delete paragraph referring to Figure 134 beginning at page 30, line 23 of the specification.

Delete paragraph referring to Figure 135 beginning at page 30, line 24 of the specification.

Delete paragraph referring to Figure 136 beginning at page 30, line 25 of the specification.

Delete paragraph referring to Figure 137 beginning at page 30, line 26 of the specification.

Delete paragraph referring to Figure 138 beginning at page 31, line 1 of the specification.

Amend paragraph referring to Figure 139 beginning at page 31, line 4 of the specification as follows:

Figure [139] 59 depicts FTMS spectrum obtained from a mixture of a 16S RNA model (10  $\mu$ M) and a 60-member combinatorial library.

Amend paragraph referring to Figure 140 beginning at page 31, line 6 of the specification as follows:

Figure [140] 60 depicts an expanded view of the 1863 complex from Figure [139] 59.

Amend paragraph referring to Figure 141 beginning at page 31, line 7 of the specification as follows:

Figure [141] 61 depicts mass of a binding ligand determined from a starting library of compounds.

Amend paragraph referring to Figure 142 beginning at page 31, line 9 of the specification as follows:

Figure [142] 62 depicts high resolution ESI-FTICR spectrum of the library used in Figures [140] 60 and [141] 61.

Amend paragraph referring to Figure 143 beginning at page 31, line 11 of the specification as follows:

Figure [143] 63 depicts use of exact mass measurements and elemental constraints to determine the elemental composition of an exemplary “unknown” binding ligand.

Amend paragraph referring to Figure 144 beginning at page 31, line 13 of the specification as follows:

Figure [144] 64 depicts ESI-MS measurements of a solution containing a fixed concentration of RNA at different concentrations of ligand.

Delete paragraph referring to Figure 145 beginning at page 31, line 15 of the specification.

Amend paragraph referring to Figure 146 beginning at page 31, line 17 of the specification as follows:

Figure [146] 65 depicts MASS screening of a 27 member library against a 27-mer RNA construct representing the prokaryotic 16S A-site.

Amend paragraph referring to Figure 147 beginning at page 31, line 19 of the specification as follows:

Figure [147] 66 depicts MS/MS of a 27-mer RNA construct representing the prokaryotic 16S A-site containing deoxyadenosine residues at the paromomycin binding site.

Amend paragraph referring to Figure 148 beginning at page 31, line 21 of the specification as follows:

Figure [148] 67 depicts MS-MS spectra obtained from a mixture of a 27-mer RNA construct representing the prokaryotic 16S A-site containing deoxyadenosine residues at the paromomycin binding and the 216 member combinatorial library respectively.

Amend paragraph referring to Figure 149 beginning at page 31, line 24 of the specification as follows:

Figure [149] 68 depicts secondary structures of the 27 base RNA models used in this work corresponding to the *18S* (eukaryotic) SEQ ID NO:382 and *16S* (prokaryotic) SEQ ID NO:35 A-sites.

Amend paragraph referring to Figure 150 beginning at page 31, line 26 of the specification as follows:

Figure [150] 69 depicts ESI-FTICR spectrum of a mixture of 27-base representations of the *16S* A-site with (7  $\mu$ M) and without (1  $\mu$ M) an 18 atom neutral mass tag attached to the 5- terminus in the presence of 500 nM paromomycin.

Amend paragraph referring to Figure 151 beginning at page 31, line 29 of the specification as follows:

Figure [151] 70 depicts mass spectra from simultaneous screening of *16S* A-site and *18S* A-site Model RNAs against a mixture of aminoglycosides.

Amend paragraph referring to Figure 152 beginning at page 31, line 31 of the specification as follows:

Figure [152] 71 depicts sequences and structures for oligonucleotides R and C.

Amend paragraph referring to Figures 153A, B and C beginning at page 32, line 1 of the specification as follows:

Figure [153A] 72A depicts mass spectrum obtained from a mixture of 5  $\mu$ M C and 125 nM paromomycin. Figure [153B] 72B depicts MS-MS spectrum obtained following isolation of  $[M-5H]^{5-}$  ions ( $m/z$  1783.6) from uncomplexed C. Figure [153C] 72C depicts MS-MS spectrum obtained following isolation of  $[M-5H]^{5-}$  ions ( $m/z$  1907.5) from C complexed with paromomycin.

Amend paragraph referring to Figures 154A and B beginning at page 32, line 6 of the specification as follows:



Figure [154A] 73A depicts MS-MS spectrum obtained from a mixture of 10  $\mu$ M C and a 216 member combinatorial library following isolation of  $[M-5H]^{5-}$  ions ( $m/z$  1919.0) from C complexed with ligands of mass  $676.0 \pm 0.6$ . Figure [154B] 73B depicts MS-MS spectrum obtained from a mixture of 10  $\mu$ M C and a 216 member combinatorial library following isolation of  $[M-5H]^{5-}$  ions ( $m/z$  1934.3) from C complexed with ligands of mass  $753.5 \pm 0.6$ .

Amend paragraph referring to Figure 155 beginning at page 32, line 11 of the specification as follows:

Figure [155] 74 depicts electrospray ionization Fourier transform ion cyclotron resonance mass spectrometry of a target / putative ligand mixture.

Amend paragraph referring to Figure 156 beginning at page 32, line 13 of the specification as follows:

Figure [156] 75 shows isotope clusters from the spectrum of Figure [155] 74.

Amend paragraph referring to Figure 157 beginning at page 32, line 14 of the specification as follows:

Figure [157] 76 depicts data tabulated and stored in a relational database.

Amend paragraph referring to Figure 158 beginning at page 32, line 15 of the specification as follows:

Figure [158] 77 shows an exemplary flow chart for a computer program for effecting certain methods in accordance with the invention.

Amend paragraph beginning at page 38, line 11 of the specification as follows:

Additional nucleic acid targets may be determined independently or can be selected from publicly available prokaryotic and eukaryotic genetic databases known to those skilled in the art. Preferred databases include, for example, Online Mendelian Inheritance in Man (OMIM), the Cancer

Genome Anatomy Project (CGAP), GenBank, EMBL, PIR, SWISS-PROT, and the like. OMIM, which is a database of genetic mutations associated with disease, was developed, in part, for the National Center for Biotechnology Information (NCBI). OMIM is publicly available through the Internet at the world wide web at, for example, [ncbi.nlm.nih.gov/Omim/](http://ncbi.nlm.nih.gov/Omim/). [OMIM can be accessed through the Internet at, for example, <http://www.ncbi.nlm.nih.gov/Omim/>.] CGAP, which is an interdisciplinary program to establish the information and technological tools required to decipher the molecular anatomy of a cancer cell. [CGAP can be accessed through the Internet at, for example, <http://www.ncbi.nlm.nih.gov/ncicgap/>.] CGAP is publicly available through the Internet at the world wide web at, for example, [ncbi.nlm.nih.gov/ncicgap/](http://ncbi.nlm.nih.gov/ncicgap/). Some of these databases may contain complete or partial nucleotide sequences. In addition, nucleic acid targets can also be selected from private genetic databases. Alternatively, nucleic acid targets can be selected from available publications or can be determined especially for use in connection with the present invention.

Amend paragraph beginning at page 38, line 25 of the specification as follows:

After a nucleic acid target is selected or provided, the nucleotide sequence of the nucleic acid target is determined and then compared to the nucleotide sequences of a plurality of nucleic acids from different taxonomic species. In one embodiment of the invention, the nucleotide sequence of the nucleic acid target is determined by scanning at least one genetic database or is identified in available publications. Preferred databases known and available to those skilled in the art include, for example, the Expressed Gene Anatomy Database (EGAD) and Unigene-Homo Sapiens database (Unigene), GenBank, and the like. EGAD contains a non-redundant set of human transcript (HT) sequences [and can be accessed through the Internet at, for example, <http://www.tigr.org/tdb/egad/egad.html>] and is publicly available through the Internet at the world wide web at, for example, [tigr.org/tdb/egad/egad.html](http://www.tigr.org/tdb/egad/egad.html). Unigene is a system for automatically partitioning GenBank sequences into a non-redundant set of gene-oriented clusters. Each Unigene cluster contains sequences that represent a unique gene, as well as related information such as the tissue types in which the gene has been expressed and map location.

Amend paragraph beginning at page 39, line 9 of the specification as follows:

In addition, Unigene contains hundreds of thousands of novel expressed sequence tag (EST) sequences. [Unigene can be accessed through the Internet at, for example, <http://www.ncbi.nlm.nih.gov/UniGene/>.] Unigene is publicly available through the Internet at the world wide web at, for example, [ncbi.nlm.nih.gov/UniGene/](http://www.ncbi.nlm.nih.gov/UniGene/). These databases can be used in connection with searching programs such as, for example, Entrez, which is known and available to those skilled in the art, and the like. [Entrez can be accessed through the Internet at, for example, <http://www.ncbi.nlm.nih.gov/Entrez/>.] Entrez is publicly available through the Internet at the world wide web at, for example, [ncbi.nlm.nih.gov/Entrez](http://www.ncbi.nlm.nih.gov/Entrez/). Preferably, the most complete nucleic acid sequence representation available from various databases is used. The GenBank database, which is known and available to those skilled in the art, can also be used to obtain the most complete nucleotide sequence. GenBank is the NIH genetic sequence database and is an annotated collection of all publicly available DNA sequences. GenBank is described in, for example, Nuc. Acids Res., 1998, 26, 1-7, which is incorporated herein by reference in its entirety, and can be accessed by those skilled in the art [through the Internet at, for example, <http://www.ncbi.nlm.nih.gov/Web/Genbank/index.html>] through the Internet at the world wide web at, for example, [ncbi.nlm.nih.gov/Web/Genbank/index.html](http://www.ncbi.nlm.nih.gov/Web/Genbank/index.html). Alternatively, partial nucleotide sequences of nucleic acid targets can be used when a complete nucleotide sequence is not available.

Amend paragraph beginning at page 39, line 24 of the specification as follows:

In another embodiment of the present invention, the nucleotide sequence of the nucleic acid target is determined by assembling a plurality of overlapping expressed sequence tags (ESTs). The EST database (dbEST), which is known and available to those skilled in the art, comprises approximately one million different human mRNA sequences comprising from about 500 to 1000 nucleotides, and various numbers of ESTs from a number of different organisms. [dbEST can be accessed through the Internet at, for example, <http://www.ncbi.nlm.nih.gov/dbEST/index.html>.] dbEST is publicly available through the Internet at the world wide web at, for example, [ncbi.nlm.nih.gov/dbEST/index.html](http://www.ncbi.nlm.nih.gov/dbEST/index.html). These sequences are derived from a cloning strategy that uses

cDNA expression clones for genome sequencing. ESTs have applications in the discovery of new genes, mapping of genomes, and identification of coding regions in genomic sequences. Another important feature of EST sequence information that is becoming rapidly available is tissue-specific gene expression data. This can be extremely useful in targeting selective gene(s) for therapeutic intervention. Since EST sequences are relatively short, they must be assembled in order to provide a complete sequence. Because every available clone is sequenced, it results in a number of overlapping regions being reported in the database.

Amend paragraph beginning at page 40, line 7 of the specification as follows:

Assembly of overlapping ESTs extended along both the 5' and 3' directions results in a full-length "virtual transcript." The resultant virtual transcript may represent an already characterized nucleic acid or may be a novel nucleic acid with no known biological function. The Institute for Genomic Research (TIGR) Human Genome Index (HGI) database, which is known and available to those skilled in the art, contains a list of human transcripts. [TIGR can be accessed through the Internet at, for example, <http://www.tigr.org/>.] TIGR is publicly available through the Internet at the world wide web at, for example, [tigr.org/](http://www.tigr.org/). The transcripts were generated in this manner using TIGR-Assembler, an engine to build virtual transcripts and which is known and available to those skilled in the art. TIGR-Assembler is a tool for assembling large sets of overlapping sequence data such as ESTs, BACs, or small genomes, and can be used to assemble eukaryotic or prokaryotic sequences. TIGR-Assembler is described in, for example, Sutton, *et al.*, *Genome Science & Tech.*, **1995**, *1*, 9-19, which is incorporated herein by reference in its entirety, [and can be accessed through the Internet at, for example, [ftp://ftp.tigr.org/pub/software/TIGR assembler](ftp://ftp.tigr.org/pub/software/TIGR_assembler)] and is publicly available through the Internet via file transfer program at, for example [tigr.org/pub.software/TIGR assembler](http://tigr.org/pub/software/TIGR assembler). In addition, GLAXO-MRC, which is known and available to those skilled in the art, is another protocol for constructing virtual transcripts. In addition, "Find Neighbors and Assemble EST Blast" protocol, which runs on a UNIX platform, has been developed by Applicants to construct virtual transcripts. Preferred steps in the Find Neighbors and Assemble EST Blast protocol is described in the flowchart set forth in Figure 2. PHRAP is used for sequence assembly within Find Neighbors and Assemble

EST Blast. [PHRAP can be accessed through the Internet at, for example, <http://chimera.biotech.washington.edu/uwgc/tools/phrap.htm>.] PHRAP is publicly available through the Internet at, for example, [chimera.biotech.washington.edu/uwgc/tools/phrap.htm](http://chimera.biotech.washington.edu/uwgc/tools/phrap.htm). One skilled in the art can construct source code to carry out the preferred steps set forth in Figure 2.

Amend paragraph beginning at page 41, line 21 of the specification as follows:

Sequence similarity searches can be performed manually or by using several available computer programs known to those skilled in the art. Preferably, Blast and Smith-Waterman algorithms, which are available and known to those skilled in the art, and the like can be used. Blast is NCBI's sequence similarity search tool designed to support analysis of nucleotide and protein sequence databases. [Blast can be accessed through the Internet at, for example, <http://www.ncbi.nlm.nih.gov/BLAST/>.] Blast is publicly available through the Internet at the world wide web at, for example, [ncbi.nlm.nih.gov/BLAST/](http://www.ncbi.nlm.nih.gov/BLAST/). The GCG Package provides a local version of Blast that can be used either with public domain databases or with any locally available searchable database. GCG Package v.9.0 is a commercially available software package that contains over 100 interrelated software programs that enables analysis of sequences by editing, mapping, comparing and aligning them. Other programs included in the GCG Package include, for example, programs which facilitate RNA secondary structure predictions, nucleic acid fragment assembly, and evolutionary analysis. In addition, the most prominent genetic databases (GenBank, EMBL, PIR, and SWISS-PROT) are distributed along with the GCG Package and are fully accessible with the database searching and manipulation programs. [GCG can be accessed through the Internet at, for example, <http://www.gcg.com/>.] GCG is publicly available through the Internet at the world wide web at, for example, [gcg.com/](http://www.gcg.com/). Fetch is a tool available in GCG that can get annotated GenBank records based on accession numbers and is similar to Entrez. Another sequence similarity search can be performed with GeneWorld and GeneThesaurus from Pangea. GeneWorld 2.5 is an automated, flexible, high-throughput application for analysis of polynucleotide and protein sequences. GeneWorld allows for automatic analysis and annotations of sequences. Like GCG, GeneWorld incorporates several tools for homology searching, gene finding, multiple sequence alignment,

secondary structure prediction, and motif identification. GeneThesaurus 1.0tm is a sequence and annotation data subscription service providing information from multiple sources, providing a relational data model for public and local data.

Amend paragraph beginning at page 42, line 22 of the specification as follows:

Another toolkit capable of doing sequence similarity searching and data manipulation is SEALS, also from NCBI. This tool set is written in perl and C and can run on any computer platform that supports these languages. [It is available for download, for example, at: <http://www.ncbi.nlm.nih.gov/Walker/SEALS/>.] It is publicly available through the Internet at the world wide web at, for example, [ncbi.nlm.nih.gov/Walker/SEALS/](http://www.ncbi.nlm.nih.gov/Walker/SEALS/). This toolkit provides access to Blast2 or gapped blast. It also includes a tool called tax\_collector which, in conjunction with a tool called tax\_break, parses the output of Blast2 and returns the identifier of the sequence most homologous to the query sequence for each species present. Another useful tool is feature2fasta which extracts sequence fragments from an input sequence based on the annotation. An exemplary use for this tool is to create sequence files containing the 5' untranslated region of a cDNA sequence.

Amend paragraph beginning at page 43, line 28 of the specification as follows:

In another embodiment of the invention, the sequences required are obtained by searching ortholog databases. One such database is Hovergen, which is a curated database of vertebrate orthologs. Ortholog sets may be exported from this database and used as is, or used as seeds for further sequence similarity searches as described above. Further searches may be desired, for example, to find invertebrate orthologs. [Hovergen can be downloaded, for example, at: <ftp://pbil.univ-lyon1.fr/pub/hovergen/>.] Hovergen is publicly available through the Internet via file transfer program at, for example, [pbil.univ-lyon1.fr/pub/hovergen/](ftp://pbil.univ-lyon1.fr/pub/hovergen/). A database of prokaryotic orthologs, COGS, is available and can be used interactively through the Internet at the world wide web at, for example, [on the internet, for example at: <http://www.ncbi.nlm.nih.gov/COG/>.

Amend paragraph beginning at page 46, line 15 of the specification as follows:

In one embodiment of the invention, secondary structure analysis is performed by alignment and covariance analysis. Numerous protocols for alignment and covariance analysis are known to those skilled in the art. Preferably, alignment is performed by ClustalW, which is available and known to those skilled in the art. ClustalW is a tool for multiple sequence alignment that, although not a part of GCG, can be added as an extension of the existing GCG tool set and used with local sequences. [ClustalW can be accessed through the Internet at, for example, <http://dot.imgen.bcm.tmc.edu:9331/multi-align/Options/clustalw.html>.] ClustalW is publicly available through the Internet at, for example, dot.imgen.bcm.tmc.edu:9331/multialign/Options/clustalw.html. ClustalW is also described in Thompson, *et al.*, *Nuc. Acids Res.*, **1994**, 22, 4673-4680, which is incorporated herein by reference in its entirety. These processes can be scripted to automatically use conserved UTR regions identified in earlier steps. Seqed, a UNIX command line interface available and known to those skilled in the art, allows extraction of selected local regions from a larger sequence. Multiple sequences from many different species can be clustered and aligned for further analysis.

Amend paragraph beginning at page 47, line 9 of the specification as follows:

Covariation is a process of using phylogenetic analysis of primary sequence information for consensus secondary structure prediction. Covariation is described in the following references, each of which is incorporated herein by reference in their entirety: Gutell, *et al.*, "Comparative Sequence Analysis Of Experiments Performed During Evolution" In Ribosomal RNA Group I Introns, Green, Ed., Austin:Landes, **1996**; Gautheret, *et al.*, *Nuc. Acids Res.*, **1997**, 25, 1559-1564; Gautheret, *et al.*, *RNA*, **1995**, 1, 807-814; Lodmell, *et al.*, *Proc. Natl. Acad. Sci. USA*, **1995**, 92, 10555-10559; Gautheret, *et al.*, *J. Mol. Biol.*, **1995**, 248, 27-43; Gutell, *Nuc. Acids Res.*, **1994**, 22, 3502-3517; Gutell, *Nuc. Acids Res.*, **1993**, 21, 3055-3074; Gutell, *Nuc. Acids Res.*, **1993**, 21, 3051-3054; Woese, *Proc. Natl. Acad. Sci. USA*, **1989**, 86, 3119-3122; and Woese, *et al.*, *Nuc. Acids Res.*, **1980**, 8, 2275-2293. Preferably, covariance software is used for covariance analysis. Preferably, Covariation, a set of programs for the comparative analysis of RNA structure from sequence alignments, is used. Covariation uses phylogenetic analysis of primary sequence information for consensus secondary

structure prediction. [Covariation can be obtained through the Internet at, for example, <http://www.mbio.ncsu.edu/RNaseP/info/programs/programs.html>.] Covariation is publicly available through the Internet at the world wide web at, for example [mbio.ncsu.edu/RNaseP/info/programs/programs.html](http://mbio.ncsu.edu/RNaseP/info/programs/programs.html). A complete description of a version of the program has been published (Brown, J. W. 1991 Phylogenetic analysis of RNA structure on the Macintosh computer. CABIOS7:391-393). The current version is v4.1, which can perform various types of covariation analysis from RNA sequence alignments, including standard covariation analysis, the identification of compensatory base-changes, and mutual information analysis. The program is well-documented and comes with extensive example files. It is compiled as a stand-alone program; it does not require Hypercard (although a much smaller 'stack' version is included). This program will run in any Macintosh environment running MacOS v7.1 or higher. Faster processor machines (68040 or PowerPC) is suggested for mutual information analysis or the analysis of large sequence alignments.

Amend paragraph beginning at page 48, line 3 of the specification as follows:

In another embodiment of the invention, secondary structure analysis is performed by secondary structure prediction. There are a number of algorithms that predict RNA secondary structures based on thermodynamic parameters and energy calculations. Preferably, secondary structure prediction is performed using either M-fold or RNA Structure 2.52. [M-fold can be accessed through the Internet at, for example, <http://www.ibc.wustl.edu/-zucker/ma/form2.cgi>] M-fold is publicly available through the Internet at the world wide web at, for example, [ibc.wustl.edu/-zucker/ma/form2.cgi](http://ibc.wustl.edu/-zucker/ma/form2.cgi) or can be downloaded for local use on UNIX platforms. M-fold is also available as a part of GCG package. RNA Structure 2.52 is a windows adaptation of the M-fold algorithm and [can be accessed through the Internet at, for example, <http://128.151.176.70/RNAstructure.html>] is publicly available through the Internet at, for example, [128.151.176.70/RNAstructure.html](http://128.151.176.70/RNAstructure.html).

Amend paragraph beginning at page 51, line 5 of the specification as follows:



In one embodiment of the invention, nucleic acids having secondary structure which correspond to the structure descriptor elements are identified by searching at least one database. Any genetic database can be searched. Preferably, the database is a UTR database, which is a compilation of the untranslated regions in messenger RNAs. A UTR database [is accessible through the Internet at, for example, <ftp://area.ba.cnr.it/pub/embnet/database/utr/>] is publicly available through the Internet via file transfer program at [area.ba.cnr.it/pub/embnet/database/utr/](ftp://area.ba.cnr.it/pub/embnet/database/utr/). Preferably the database is searched using a computer program, such as, for example, Rnamot, a UNIX-based motif searching tool available from Daniel Gautheret. Each “new” sequence that has the same motif is then queried against public domain databases to identify additional sequences. Results are analyzed for recurrence of pattern in UTRs of these additional ortholog sequences, as described below, and a database of RNA secondary structures is built. One skilled in the art is familiar with Rnamot. Briefly, Rnamot takes a descriptor string, such as the one shown in Figure 9, and searches any Fasta format database for possible matches. Descriptors can be very specific, to match exact nucleotide(s), or can have built-in degeneracy. Lengths of the stem and loop can also be specified. Single stranded loop regions can have a variable length. G-U pairings are allowed and can be specified as a wobble parameter. Allowable mismatches can also be included in the descriptor definition. Functional significance is assigned to the motifs if their biological role is known based on previous analysis. Known regulatory regions such as Iron Response Element have been found using this technique (see, Example 1 below). In embodiments of the invention in which a database containing prokaryotic molecular interaction sites is compiled, it is preferable to refrain from searching human sequences or, alternatively, discarding human sequences when found.

Amend paragraph beginning at page 71, line 13 of the specification as follows:

Using DOCK, ligands have been identified for certain protein targets. Recent efforts in this area have resulted in reports of the use of DOCK to identify and design small molecule ligands that exhibit binding specificity for nucleic acids such as RNA double helices. While RNA plays a significant role in many diseases such as AIDS, viral and bacterial infections, few studies have been

made on small molecules capable of specific RNA binding. Compounds possessing specificity for the RNA double helix, based on the unique geometry of its deep major groove, were identified using the DOCK methodology (Chen *et al.*, *Biochemistry*, **1997**, *36*, 11402; Kuntz *et al.*, *Acc. Chem. Res.*, **1994**, *27*, 117). Using a recent X-ray structure for r(UAAGGAGGUGAU).r(AUCACCUCCUUA) [(SEQ ID NO:359)] (SEQ ID NO:52) as the model structure for the A-form RNA duplex, DOCK identified several aminoglycosides as candidate ligands, characterized by shape complementarity to the RNA groove. Binding experiments then revealed that one of these aminoglycosides not only bound preferentially to RNA over B-form DNA but also that the ligand binds in the targeted RNA major groove. Recently, the application of DOCK to the problem of ligand recognition in DNA quadruplexes has also been reported (Chen *et al.*, *Proc. Natl. Acad. Sci.*, **1996**, *93*, 2635).

Delete paragraph beginning at page 72, line 28 of the specification.

Delete pages 73-88 of the specification.

Delete paragraph beginning at page 88, line 18 of the specification.

Delete paragraph beginning at page 89, line 3 of the specification.

Amend paragraph beginning at page 140, line 5 of the specification as follows:

The preferred model system employed herein comprises a library comprised of five 2-deoxystreptamine aminoglycoside antibiotics which have a range of binding affinities for the decoding sites of the prokaryotic and eukaryotic ribosomal RNA ranging from ~28 nM to ~1.5 mM. Figure [149] 68 illustrates the secondary structures for the 27-nucleotide models of the 16S and 18S rRNA decoding sites. These constructs consist of a 7 base pair stem structure containing a non-canonical U-U and a purine-adenosine mismatch base pair adjacent to a bulged adenosine residue

closed by a UUCG tetraloop. NMR studies of a complex between 16S and paromomycin show that the RNA makes primary hydrogen bond, electrostatic, and stacking contacts with the aminoglycoside (Fourmy, *et al.*, *Science*, **1996**, 274, 1367-1371) and that paromomycin binds in the major groove of the model A-site RNA within the pocket created by the A-A base pair and the single bulged adenine. The masses for the two RNA models differ by only 15.011 Da and the  $(M-5H^+)^{5-}$  species of these constructs differ by only 3 m/z units. While the high resolution capabilities of the FTICR mass spectrometer can easily resolve these species, mass spectra from a solution containing both RNAs are complicated by overlap among the signals from free RNA ions and their sodium and potassium-adducted species.

Amend paragraph beginning at page 141, line 9 of the specification as follows:

While the ability to shift the m/z range of closely related macromolecules is highly desirable as described above, it is preferably desired that the mass tag does not alter key physical properties of the target or the ligand binding properties. Preferably, an 18-atom mass tag ( $C_{12}H_{25}O_9$ ) attached to the 5'-terminus of the RNA oligomer through a phosphodiester linkage can be employed. This mass tag has no appreciable affect on oligonucleotide solubility, ionization efficiency, or UV absorbance, and does not alter RNA-ligand binding. This latter attribute is evidenced by the data in Figure [150] 69 that illustrates the conserved ratio of free:bound RNA for the untagged and tagged RNA models of the bacterial decoding site under competitive binding conditions with paromomycin.

Amend paragraph beginning at page 141, line 28 of the specification as follows:

The ESI-FTICR mass spectrum depicted in Figure [151] 70 was acquired from a 10 mM mixture of untagged 16S and tagged 18S in the presence of an equimolar mixture of five aminoglycosides. It is to be understood that other biomolecules may be used in place of the aminoglycosides. The aminoglycosides have been selected from two classes of 2-deoxystreptamines: 4,5-disubstituted (paromomycin, and lividomycin), and 4,6-disubstituted (tobramycin, sisomicin, and bekanamycin), present at 500 nM each. Complexes corresponding to 1:1 binding of individual aminoglycosides were observed between 16S and all members of the aminoglycoside mixture, with

the apparent affinities estimated from the abundances of the respective complexes differing substantially. Signal intensities from the complexes with paromomycin ( $m/z$  1925.572) and lividomycin ( $m/z$  1954.790) are consistent with MS-measured dissociation constants of 110 nM and 28 nM, respectively. The intensities of 16S complexes with tobramycin ( $m/z$  1895.960), bekanamycin ( $m/z$  1899.171), and sisomicin ( $m/z$  1891.972) were reduced, consistent with solution dissociation constants of  $\sim 1.5$  mM. Wang, *et al.*, *Biochemistry*, **1997**, 36, 768-779. Hence, under these assay conditions, the MS-observed ion abundances reflect the solution dissociation constants. The inset in Figure [151] 70 demonstrates the ability to resolve the isotopic envelope for each complex and allows mass differences to be calculated from homo-isotopic species, thus, measuring the difference in  $m/z$  between the RNA target and the RNA-ligand complex allows precise mass determination of the ligand. The spectrum is calibrated using multiple isotope peaks of the  $(M-5H^+)^{5-}$  and  $(M-4H^+)^{4-}$  charge states of the free RNA as internal mass standards which brackets the  $m/z$  range in which complexes are observed. The average mass measurement error obtained for the complexes in Figure [151] 70 is 2.1 ppm when  $m/z$  differences are measured between the most abundant ( $4^{13}C$ ) isotope peak of 16S and each complex. This post calibration scheme is easily automated which enables rapid, high precision mass measurements of affinity selected ligands against multiple targets in a high throughput mode.

Amend paragraph beginning at page 142, line 22 of the specification as follows:

The enhanced affinity of lividomycin for 16S relative to the affinity of paromomycin for 16S is interesting. While lividomycin is believed to bind to the 16S ribosomal subunit, the exact site of interaction has not been established. Lividomycin has two significant structural differences from paromomycin. First, the additional mannopyranosyl ring could generate new macromolecular contacts with the RNA. However, the orientation of paromomycin ring IV is disordered in the NMR-derived structure for the complex with 16S. In addition, a hydroxyl group on ring I that makes a contact with A1492 is missing. The relatively high abundance of the 16S-lividomycin complex suggests that lividomycin binds at or near the 16S A-site, and generates additional contacts that enhance the binding affinity nearly 4-fold. Perhaps the most striking feature of the spectrum in

Figure [151] 70 is the complete absence of complexes between 18S and paromomycin or lividomycin. This result suggests there must be poor shape and electrostatic complementarity between the 4,5-disubstituted 2-DOS class of aminoglycoside and the conserved architecture of the eukaryotic ribosomal decoding site.

Amend paragraph beginning at page 144, line 3 of the specification as follows:

In other preferred embodiments, the nucleic acid fragment comprise the consensus sequence NNNNCNNNNNNNUNNANNNNNNNN (SEQ ID NO:1) or NNNNCNNNNNNNUNNANNNNNN NNN [(SEQ ID NO:384)] (SEQ ID NO:65) and wherein the sequence has a first double stranded region, an internal loop region, a second double stranded region and an end loop region. In other preferred embodiments, an *in silico* representation of a nucleic acid fragment that is conserved across at least two species comprises the consensus sequence NNNNCNNNNNNNUNNANNNNNNNN (SEQ ID NO:1) or NNNNCNNNNNNNUNNANNNNNNNN [(SEQ ID NO:384)] (SEQ ID NO:65). In other preferred embodiments, a purified and isolated nucleic acid fragment that is conserved across at least two species comprises the sequence NNNNCNNNNNNNUNNANNNNNNNN [(SEQ ID NO:1)] (SEQ ID NO:1) or NNNNCNNNNNNNUNNANNNNNNNN [(SEQ ID NO:384)] (SEQ ID NO:65). In other preferred embodiments, a purified and isolated nucleic acid fragment comprises the human sequence (SEQ ID NO:2) UUUACAACAUAUAUCUAGUUUACAGAAAAAUC. In other preferred embodiments, an *in silico* representation of a nucleic acid fragment comprises the human sequence UUUACAACAUAUAUCUAGUUUACAGAAAAAUC (SEQ ID NO:2).

Amend paragraph beginning at page 145, line 19 of the specification as follows:

In other preferred embodiments, the nucleic acid comprises the consensus sequence NNNNANAUGGGNNNUCACANNUANCUGUGUCCUAUGGAAACUNNUUN (SEQ ID NO:3), NNNNANAUGGGNNNUCACANNUACUGUGUCCUAUGGAAACUNNUUN [(SEQ ID NO:385)] (SEQ ID NO:66), NNNNANAUGGGNNNUCACANNUACUGUGUCCUAUGGAAACUNNUUN [(SEQ ID NO:386)] (SEQ ID NO:67), NNNNANAUGGGNNNUCACANNUACUGUGUCCUAUGGAAACUUUN [(SEQ ID NO:387)] (SEQ ID NO: 68), NNNNANAUGGGNNN

UCACANNUANCUGUGUCCUAUGGAAACUNUUN [(SEQ ID NO:388)] SEQ ID NO: 69,  
 NNNNANAUGGGNNNUCACANNUANCUGUGUCCUAUGGAAACUUUN [(SEQ ID  
 NO:389)] (SEQ ID NO:70), NNNNANAUGGGNNNUCACANNUANCUGUGUCCUAUGGAA  
 ACUNNUUN [(SEQ ID NO:390)] (SEQ ID NO:71), NNNNANAUGGGNNNUCACANNUACUG  
 UGUCCUAUGGAAACUNNUUN [(SEQ ID NO:391)] (SEQ ID NO:72),  
 NNNNANAUGGGNNNUCACANNUACUGUGUCCUAUGGAAACUNUUN [(SEQ ID NO:392)]  
(SEQ ID NO:73), NNNNANAUGGGNNNUCACANNUACUGUGUCCUAUGGAAACUUUN  
 [(SEQ ID NO:393)] SEQ ID NO:74, NNNNANAUGGGNNNUCACANNUANCUGUGUCCUAU  
 GGAAACUNUUN [(SEQ ID NO:394)] (SEQ ID NO: 75), NNNNANAUGGGNNNUCACANNUAN  
 CUGUGUCCUAUGGAAACUUUN [(SEQ ID NO:395)] (SEQ ID NO:76),  
 NNNNANAUGGGNNNUCACANNUANCUGUGUCCUAUGGAAACUNNUUN [(SEQ ID  
 NO:396)] (SEQ ID NO:77), NNNNANAUGGGNNNUCACANNUACUGUGUCCUAUGGAAACU  
 NNUUN [(SEQ ID NO:397)] (SEQ ID NO:78), NNNNANAUGGGNNNUCACANNUACUGUGU  
 CCUAUGGAAACUNUUN [(SEQ ID NO:398)] (SEQ ID NO: 79), NNNNANAUGGGNNUCACA  
 NNUACUGUGUCCUAUGGAAACUUUN [(SEQ ID NO:399)] (SEQ ID NO:80),  
 NNNNANAUGGGNNNUCACANNUANCUGUGUCCUAUGGAAACUNUUN [(SEQ ID NO:400)]  
(SEQ ID NO:81), NNNNANAUGGGNNNUCACANNUANCUGUGUCCUAUGGAAACUUUN  
 [(SEQ ID NO:401)] (SEQ ID NO:82), NNNNANAUGGGNNNUCACANNUANCUGUGUCCUAU  
 GGAAACUNNUUN [(SEQ ID NO:402)] (SEQ ID NO:83), NNNNANAUGGGNNNUCACANNUAC  
 UGUGUCCUAUGGAAACUNNUUN [(SEQ ID NO:403)] (SEQ ID NO: 84),  
 NNNNANAUGGGNNNUCACANNUACUGUGUCCUAUGGAAACUNUUN [(SEQ ID NO:404)]  
(SEQ ID NO:85), NNNNANAUGGGNNNUCACANNUACUGUGUCCUAUGGAAACUUUN [(SEQ  
 ID NO:405)] (SEQ ID NO:86), NNNNANAUGGGNNNUCACANNUANCUGUGUCCUAUGGAAA  
 CUNUUN [(SEQ ID NO:406)] (SEQ ID NO: 87), or NNNNANAUGGGNNNUCACANNUANCUGUG  
 UCCUAUGGAAACUUUN [(SEQ ID NO:407)] (SEQ ID NO:88) and having a first double  
 stranded region, a first internal loop region, a second double stranded region, a second internal loop  
 region, a third double stranded region and an end loop region. In other preferred embodiments, a  
 purified and isolated nucleic acid fragment comprises the human sequence (SEQ ID NO:4)

UAGGAUAUGGGUCACACUUAUCUGUGUUCCUAUGGAAACUAUUUG. In other preferred embodiments, a purified and isolated nucleic acid fragment comprises the mouse sequence (SEQ ID NO:5) UAGGAGAUGGGGGUCACACUACUGUGUUCCUAUGGAAACUUUG. In other preferred embodiments, a purified and isolated nucleic acid fragment comprises the rat sequence (SEQ ID NO:6) UAGGAGAUGGGGGGUCACACUACUGUGUUCCUAUGAAACUUUUG.

Amend paragraph beginning at page 146, line 26 of the specification as follows:

In other preferred embodiments, a nucleic acid comprises the consensus sequence AUGG GNNNUCACANNUANCUGUGUUCCUAU (SEQ ID NO:7), AUGGGNNNUCACANNUACUG UGUUCCUAU [(SEQ ID NO:408)] (SEQ ID NO:89), AUGGGNNNUCACANNUANCUGUGU CCUAU [(SEQ ID NO:409)] (SEQ ID NO:90), AUGGGNNNUCACANNUACUGUGUUCCUAU [(SEQ ID NO:410)] (SEQ ID NO:91), AUGGGNUCACANNUANCUGUGUUCCUAU [(SEQ ID NO:411)] (SEQ ID NO:92), AUGGGNUCACANNUACUGUGUUCCUAU [(SEQ ID NO:412)] (SEQ ID NO:93), AUGGGUCACANNUANCUGUGUUCCUAU [(SEQ ID NO:413)] (SEQ ID NO:94), or AUGGGUCACANNUACUGUGUUCCUAU [(SEQ ID NO:414)] (SEQ ID NO:95) and having a first double stranded region, an internal loop region, a second double stranded region and an end loop region. A purified and isolated nucleic acid fragment comprising the human sequence (SEQ ID NO:8) AUGGGUCACACUUAUCUGUGUUCCUAU. In other preferred embodiments, a purified and isolated nucleic acid fragment comprising the mouse sequence (SEQ ID NO:9) AUGGGGGUCACACUACUGUGUUCCUAU. In other preferred embodiments, a purified and isolated nucleic acid fragment comprising the rat sequence (SEQ ID NO:10) AUGGGGGGU CACACUACUGUGUUCCUAU.

Amend paragraph beginning at page 151, line 16 of the specification as follows:

In other preferred embodiments, a nucleic acid comprising the consensus sequence NNUNNNNNNNGAUCNUNNNNGAUNCUUUNUNNNANCCNNNNNNNN (SEQ ID NO:20), NNUNNNNNNNGAUCNUNNNNGAUNCUUUNUNNNANCCNNNNNNNN [(SEQ ID NO:415)] (SEQ ID NO: 96), or NNUNNNNNNNGAUCNUNNNNGAUNCUUUNUNNNACCNNNNNNNN

[(SEQ ID NO:416)] (SEQ ID NO:97) and having a first double stranded region, a first internal loop region, a second double stranded region, and a first end loop region, a third double stranded region, and a second end loop region. In other preferred embodiments, a purified and isolated nucleic acid fragment comprising the human sequence (SEQ ID NO:21) UAUAAUAUGGAUCUUUAUG AUUCUUUUUGUAAGCCCUAGGGGC. In other preferred embodiments, a purified and isolated nucleic acid fragment comprising the mouse or rat sequence (SEQ ID NO:22) GAUAAUAUGGAUCUUUAAAGAUUCUUUUUGUAAGCCCCAAGGGC.

Amend paragraph beginning at page 152, line 9 of the specification as follows:

In preferred embodiments, the nucleotides forming the first side of the first double stranded region are of the sequence NNNGA, UAAGA, AAAGA, UAUGA, or UUUGA and the nucleotides forming the second side of the first doubled stranded region are of the sequence [GNGNN, GGGCU, or GCGUG] UUNNG, UUUUG, or UUCUG. In other preferred embodiments, the nucleotides forming the first end loop region are of the sequence UNCU, UUCU, or UCCU. In other preferred embodiments, the nucleotides forming the first side of the second double stranded region are of the sequence AGCCC and the nucleotides forming the second side of the second doubled stranded region are of the sequence GNGNN, GGGCU, or GCGUG. In other preferred embodiments, the nucleotides forming the second end loop region are of the sequence NAN, UAC, UAG, CAA, or UAA. Preferably, the nucleic acid comprises a portion of interleukin-2 RNA. More preferably, the nucleic acid comprises a portion of the 3' UTR of interleukin-2 mRNA.

Amend paragraph beginning at page 159, line 4 of the specification as follows:

An alternate, and preferred, approach to finding orthologs is the use of Hovergen database and query tools that have been described in Duret, *et al.*, *Nuc. Acids Res.*, **1994**, 22, 2360-2365, which is incorporated herein by reference in its entirety. [The use of] Hovergen was used to identify related sequences [is shown in Figure 55] (tree classification at the species level []) and Figure 56 ([]) and classification at the order level). Sequences corresponding to each of these orthologs was saved in GenBank format and grouped together in a single data file. Untranslated regions in both the 5'



and 3' flanks of the coding region was extracted using SEALS and COWX, as shown in Figure [57] 55.

Amend paragraph beginning at page 159, line 13 of the specification as follows:

The IRE sequences are more constrained because they form an important structure. Thus, they stand out better and can be more readily identified even in closely related sequences. However, for this to work for any gene, the compare algorithm has been rewritten (see, Figures 5A-C). This new tool, CompareOverWins, allows a dynamic selection of both the range of window sizes, as well the hit threshold. This algorithm needs as its input parsed and separated 5' and 3' UTR sequences. Tools available within the Seals genome analysis package described earlier can be used to achieve this. Figure [57] 55 describes the steps involved.

Amend paragraph beginning at page 159, line 20 of the specification as follows:

To identify the IRE [iron responseve element] using the methods described herein, the compare over windows [widows] algorithm was used and the results visualized using AlignHits (Figure 5D for the algorithm). [Representative results are shown in Figure 62.] In addition to optimizing the thresholding, CompareOverWins also extracts the sequence corresponding to the hits. ClustalW (version 1.74) was used on the extracted sequences to create a locally gapped alignment [(see, Figure 63)]. A representative flow scheme for this approach is shown in Figure 56 [64].

Amend paragraph beginning at page 159, line 28 of the specification as follows:

Sets of sequences that show evidence of conservation in orthologs and paralogs or other related genes are analyzed for the ability to form internal structure. This is accomplished by analyzing each sequence in a matrix where the sequeunce is plotted 5' to 3' on the X axis and its complement is plotted 5' to 3' on the Y axis, such as in, for example, self-complementary analysis. Matches that correspond to potential intramolecular base pairs are scored according to a table of values. When the human ferritin IRE sequence is analyzed in this fashion, the diagonals indicate potential self- complementary regions. Each of the 13 IRE sequences described in this example were

analyzed in the same fashion. While each of the sequences can form a variety of different structures, the structure most likely to occur is one common to all the sequences. By superimposing the plots of all 13 individual sequences [(see, Figure 65)], the potential structure common to all the sequences is deduced.

Amend paragraph beginning at page 160, line 10 of the specification as follows:

The above scheme has been implemented algorithmically into a program called RevComp (see, Figure 53). RevComp creates a sorted list of all the structures. Representative results can be viewed either as a “dome” output [(see, Figure 66)] or as a “connect” or “ct” file which can be used in one of many RNA structure viewing programs (RNAStructure, RNAViz, etc.). [A representative example of such a structure drawing is shown in Figure 67].

Amend paragraph beginning at page 160, line 22 of the specification as follows:

Phylogenetic [Figures 68 and 69 represent phylogenetic] tree outputs for all Histone orthologs in Hovergen database was obtained. Each of these orthologs was saved in GenBank format and grouped together in a single data file. Untranslated regions in both the 5' and 3' flanks of the coding regions were extracted and compared using SEALS and COWX as described earlier (see, Figures 55 [57] and 56 [64]).

Amend paragraph beginning at page 160, line 27 of the specification as follows:

Following extraction and comparison by SEALS and COWX, Align Hits was used to determine potentially interesting regions [(see, Figure 70). One such region is shown encircled]. The sequences corresponding to the region of interest was extracted from all species for alignment with CLUSTAL W (1.74). Following extraction of sequence information from Align Hits, CLUSTAL W (1.74) was used to provide multiple sequence alignment shown [(see, Figure 71)]. Each of the putative hit sequences was analyzed for the ability to form internal structure. This was accomplished by analyzing each sequence in a matrix where the sequence was plotted 5' to 3' on the X axis and its complement is plotted 5' to 3' on the Y axis. Base-pairs along the diagonals indicate

potential self-complementary regions that can form secondary structures. [Figure 72 shows a representative reverse complement matrix. Figure 73 shows a] A representative sequence alignment in a dome format can show [showing] potential stem formation between the base pairs. Following conversion of the dome format file to a ct file, RNA Structure 3.21 is used to visualize the structure [(see, Figure 74)].

Amend paragraph beginning at page 161, line 11 of the specification as follows:

Vimentin is an intermediate filament protein whose 3'UTR is highly conserved between species. Previous studies by Zehner *et al.*, (*Nuc. Acids Res.*, **1997**, 25, 3362-3370) has shown that a proposed a complex stem-loop structure contained within this region may be important for vimentin mRNA functions such as mRNA localization. The same region was identified using the present analysis, thus validating the present approach. In addition, based on the analyses described herein, a second stem-loop structure that occurs downstream of the previously proposed structure that may have a role in regulating vimentin fuction as well has been identified [(see, Figure 75).]

Amend paragraph beginning at page 161, line 19 of the specification as follows:

A representative phylogenetic tree output for all Vimentin orthologs in Hovergen database was obtained [is shown in Figure 76]. Each of these orthologs was saved in GenBank format and grouped together in a single data file. Untranslated regions in both the 5' and 3' flanks of the coding regions were extracted and compared using SEALS and COWX as described earlier (see, Figures 55 [57] and 56 [64]).

Amend paragraph beginning at page 161, line 24 of the specification as follows:

Following extraction and comparison by SEALS and COWX, Align Hits was used to determine potentially interesting regions. Two such regions appeared, and were used for subsequent analyses [(see, Figure 77)]. Following extraction of sequence information from Align Hits for the first region [1], CLUSTAL W was used to provide multiple sequence alignment [shown (see, Figure 78)]. Potential stem formation between base pairs was [is] given above the sequence alignment in a

dome format [is shown in Figure 79]. Following conversion of the dome format file to a ct file, RNA Structure 3.21 was used to visualize the structure [(see, Figure 80)]. This structure is very similar to the one proposed by Zehner *et al.* [(see, Figure 81).] Zehner *et al.* presented a detailed chemical analysis of their proposed structure for the minimal binding domain in the 3' UTR of Vimentin. This analysis included cleavage with single-strand-specific (ChS or T1) or double-strand-specific (V1) nucleases as well as after exposure to lead acetate.

Amend paragraph beginning at page 162, line 6 of the specification as follows:

Following extraction of sequence information from Align Hits for the second region [2], CLUSTAL W was used to provide multiple sequence alignment [shown in Figure 82]. The potential stem formation between base pairs in the second region [2] was [is] given above the sequence alignment in a dome format [(see, Figure 83)]. Following conversion of the dome format file to a ct file, RNA Structure 3.21 was used to visualize the structure for the second region [2 (see, Figure 85)].

Amend paragraph beginning at page 162, line 19 of the specification as follows:

A representative phylogenetic tree output for all Transferrin receptor orthologs in Hovergen database was obtained [is shown in Figure 84]. Each of these orthologs was saved in GenBank format and grouped together in a single data file. Untranslated regions in both the 5' and 3' flanks of the coding region were extracted and compared using SEALS and COWX as described earlier (see, Figures 55 [57] and 56 [64]).

Amend paragraph beginning at page 162, line 24 of the specification as follows:

Following extraction and comparison by SEALS and COWX, Align Hits was used to determine potentially interesting regions, [as shown in Figure 85. This can be seen where a vertical line intersects a series of horizontal lines representing sequence information from a set of species. This] The first region, between base pairs 920 to 990, in the 3 prime UTR of transferrin receptor was extracted from all species for alignment with CLUSTAL W (1.74).

Amend paragraph beginning at page 162, line 29 of the specification as follows:

Following extraction of sequence information from Align Hits for the first region [1], CLUSTAL W (1.74) was used to provide multiple sequence alignment [as shown in Figure 86]. A representative potential stem formation between base pairs was [is] given above the sequence alignment in a dome format [as shown in Figure 87]. Following conversion of the dome format file to a ct file, RNA Structure 3.21 was used to visualize the structure. [(see, Figure 88). This can be seen where a vertical line intersects a series of horizontal lines representing sequence information from a set of species. This] The second region, between base pairs 990 to 1050, in the 3 prime UTR of transferrin receptor was extracted from all species for alignment with CLUSTAL W (1.74) [(see, Figure 89)].

Amend paragraph beginning at page 163, line 8 of the specification as follows:

Following extraction of sequence information from Align Hits for the second region [2], CLUSTAL W (1.74) was used to provide multiple sequence alignment [as shown in Figure 90]. Potential stem formation between base pairs was [is] given above the sequence alignment in a dome format [as shown in Figure 91]. Following conversion of the dome format file to a ct file, RNA Structure 3.21 was used to visualize the structure [as shown in Figure 92]. Following extraction and comparison by SEALS and COWX, Align Hits was used to determine potentially interesting regions. [This can be seen where a vertical line intersects a series of horizontal lines representing sequence information from a set of species. This] The third region, between base pairs 1372 to 1423, in the 3 prime UTR of transferrin receptor was extracted from all species for alignment with CLUSTAL W (1.74) [(see, Figure 93)].

Amend paragraph beginning at page 163, line 18 of the specification as follows:

Following extraction of sequence information from Align Hits for the third region [3], CLUSTAL W (1.Ex.34) was used to provide multiple sequence alignment [as shown in Figure 94]. Potential stem formation between base pairs was [is] given above the sequence alignment in a dome format [as shown in Figure 95]. Following conversion of the dome format file to a ct file, RNA

Structure 3.21 was used to visualize the structure [as shown in Figure 96]. Following extraction and comparison by SEALS and COWX, Align Hits was used to determine potentially interesting regions. [This can be seen where a vertical line intersects a series of horizontal lines representing sequence information from a set of species. This] The fourth region, between base pairs 1439 to 1479, in the 3 prime UTR of transferrin receptor was extracted from all species for alignment with CLUSTAL W (1.74) [(see, Figure 97)].

Amend paragraph beginning at page 163, line 28 of the specification as follows:

Following extraction of sequence information from Align Hits for the fourth region [4], CLUSTAL W (1.Ex.34) was used to provide multiple sequence alignment [as shown in Figure 98]. Potential stem formation between base pairs was [is] given above the sequence alignment in a dome format [is shown in Figure 99]. Following conversion of the dome format file to a ct file, RNA Structure 3.21 was used to visualize the structure [as shown in Figure 100]. Following extraction and comparison by SEALS and COWX, Align Hits was used to determine potentially interesting regions. [This can be seen where a vertical line intersects a series of horizontal lines representing sequence information from a set of species. This] The fifth region, between base pairs 1479 to 1542, in the 3 prime UTR of transferrin receptor was extracted from all species for alignment with CLUSTAL W (1.74) [(see, Figure 101)].

Amend paragraph beginning at page 164, line 7 of the specification as follows:

Following extraction of sequence information from Align Hits for the fifth region [5], CLUSTAL W (1.Ex.34) was used to provide multiple sequence alignment [as shown in Figure 102]. Potential stem formation between base pairs was [is] given above the sequence alignment in a dome format [is shown in Figure 103]. Following conversion of the dome format file to a ct file, RNA Structure 3.21 was used to visualize the structure [as shown in Figure 104].

Amend paragraph beginning at page 164, line 13 of the specification as follows:

Ornithine decarboxylase (ODC) is the first enzyme in the polyamine biosynthetic pathway. Studies have shown existence of translational regulatory elements both in the 5' and 3' untranslated regions (Grens *et al.*, *J. Biol. Chem.*, **1990**, 265, 11810). Secondary structures have been proposed to exist in both these regions, though there is no conclusive evidence for it. The methods described herein identified two structures in the 3' UTR, as shown below. The presence of one of these structures [(see, Figure 105)] was verified using mass spectrometry probing (Griffey, *et al.*, *Proc. SPIE-Int. Soc. Opt. Eng.*, 2985 (Ultrasensitive Biochemical Diagnostics II): 82-86, which is incorporated herein by reference in its entirety). Two representative sequences that showed slight variation in their lengths [(see, Figure 106)] were made into RNA and subjected to MS structure probing. Results [shown in Figure 66] confirm the presence of a stem-loop structure. Accordingly, identification of a novel secondary structure can be identified from the methods described herein, and such existence has been independently verified by structure probing.

Amend paragraph beginning at page 164, line 26 of the specification as follows:

Phylogenetic tree outputs for all Ornithine Decarboxylase orthologs in Hovergen database were obtained [is shown in Figure 107 and Figure 108]. Each of these orthologs was saved in GenBank format and grouped together in a single data file. Untranslated regions in both the 5' and 3' flanks of the coding region were extracted and compared using SEALS and COWX as described earlier (see, Figures 55 [57] and 56 [64]).

Amend paragraph beginning at page 165, line 1 of the specification as follows:

Following extraction and comparison by SEALS and COWX, Align Hits was used to determine potentially interesting regions [as shown in Figure 109]. Two such regions appeared [appear], and were used for subsequent analyses. Following extraction of sequence information from the first region [1], CLUSTAL W (1.74) was used to provide multiple sequence alignment shown. Each of the putative hit sequences was analyzed for the ability to form internal structure [as shown] in a [the] reverse complement matrix [depicted in Figure 110]. This was accomplished by analyzing each sequence in a matrix where the sequence is plotted 5' to 3' on the X axis and its complement is

plotted 5' to 3' on the Y axis. Base-pairs along the diagonals indicate potential self- complementary regions that can form secondary structures. Domes view of the potential stem formation between base pairs in region 1 is given above the sequence alignment was determined using RevComp [(see, Figure 111)]. RNA Structure 3.2 was used to visualize the structure [(see, Figure 112)].

Amend paragraph beginning at page 165, line 13 of the specification as follows:

Mass spectrometry analyses techniques were used to probe for structure. The cluster alignment of the first region of ornithine decarboxylase 3' UTR [Figure 106] showed presence of gaps/inserts in the multiple alignment. Two representative RNAs (gi404561 and gi35135) from the alignments [shown in Figure 106] were used for this experiment. Analysis of the pattern of induced fragmentation showed a very strong likelihood for base-pairing along the top half of the stem-loop structure [(shown inverted in the figure)]. This corresponds to bases 11-14 and 20-23 in 404561 or bases 8-11 and 18-21 in 35135. Bulged bases (G9 in 404561 or U22 in 35135) also showed characteristic fragmentation pattern. The bottom-half of the structure appeared to be less stable, and showed some fragmentation where our analyses had predicted base-pairing. This was particularly true in the sequence 35135. This region, however, has several contiguous A-U or G-U base-pairs which tend to be less stable, and therefore have a higher probability of fragmentation.

Amend paragraph beginning at page 165, line 24 of the specification as follows:

Following extraction of sequence information from Align Hits for the second region [2], CLUSTAL W was used to provide multiple sequence alignment [shown as shown in Figure 113]. Potential stem formation between base pairs in the second region [2] was [is] given above the sequence alignment in a dome format [as shown in Figure 114]. Following conversion of the dome format file to a ct file, RNA Structure 3.21 was used to visualize the structure for the second region [2 as shown in Figure 115].

Amend paragraph beginning at page 166, line 2 of the specification as follows:



A representative phylogenetic tree output for all IL-2 orthologs in Hovergen database was obtained [is shown in Figure 116]. Each of these orthologs was saved in GenBank format and grouped together in a single data file. Untranslated regions in both the 5' and 3' flanks of the coding region were extracted and compared using SEALS and COWX as described earlier (*see*, Figures 55 [57] and 56 [64]).

Amend paragraph beginning at page 166, line 7 of the specification as follows:

Following extraction and comparison by SEALS and COWX, Align Hits was used to determine potentially interesting regions in the 3'UTR region. Two such regions appear, and were used for subsequent analyses [(*see*, Figure 117)]. Following extraction of sequence information from Align Hits for the first region [1], CLUSTAL W (1.74) was used to provide multiple sequence alignment [shown in Figure 118]. Domes view of the potential stem formation between base pairs in the first region [1 is] was given above the sequence alignment [was determined] using RevComp [(*see*, Figure 119)]. RNA Structure 3.2 was used to visualize the structure [as depicted in Figure 120]. Following extraction of sequence information from Align Hits for the second region [2], CLUSTAL W (1.74) was used to provide multiple sequence alignment [shown in Figure 121]. Potential stem formation between base pairs in the second region was [2 is] given above the sequence alignment in a dome format [as shown in Figure 122]. Following conversion of the dome format file to a ct file, RNA Structure 3.21 was used to visualize the structure for the second region [2 as shown in Figure 123].

Amend paragraph beginning at page 166, line 20 of the specification as follows:

In addition to the two regions described above, a third region, downstream of, and partially overlapping the second region [2], was identified using an alternate reference sequence (3087784.fa) [and is shown in Figure 124]. Following extraction of sequence information from Align Hits for this region, CLUSTAL W (1.74) was used to provide multiple sequence alignment [shown in Figure 125]. Potential stem formation between base pairs in the third region [3] is shown in Figure 57 [126] above the sequence alignment in a dome format. Following conversion of the dome format file

to a ct file, RNA Structure 3.21 was used to visualize the structure for the third region [3] (*see*, Figure 58 [127]).

Amend paragraph beginning at page 166, line 29 of the specification as follows:

Representative phylogenetic tree output for all IL-4 orthologs in Hovergen database was obtained [is shown in Figure 128]. Each of these orthologs was saved in GenBank format and grouped together in a single data file. Untranslated regions in both the 5' and 3' flanks of the coding region were extracted and compared using SEALS and COWX as described earlier (*see*, Figures 55 [57] and 56 [64]).

Amend paragraph beginning at page 167, line 4 of the specification as follows:

Following extraction and comparison by SEALS and COWX, Align Hits was used to determine potentially interesting regions in the 5'UTR region [as shown in Figure 129]. Following extraction of sequence information from Align Hits for the above region, CLUSTAL W (1.74) was used to provide multiple sequence alignment [shown in Figure 130]. Domes view of the potential stem formation between base pairs in the region was [is] given above the sequence alignment [was determined] using RevComp [*see*, Figure 131)]. RNA Structure 3.2 was used to visualize the structure [as shown in Figure 132].

Amend paragraph beginning at page 167, line 11 of the specification as follows:

[Figure 133 depicts a representative] Align Hits was used to view [of] hits in the 3'UTR region of IL-4. Following extraction of sequence information from Align Hits for the 3' UTR region, CLUSTAL W (1.74) was used to provide multiple sequence alignment [as shown in Figure 134]. Potential stem formation between base pairs in the second region [2 is] was given above the sequence alignment in a dome format [is shown in Figure 135]. Following conversion of the dome format file to a ct file, RNA Structure 3.21 was used to visualize the structure for the second region [2 (*see*, Figure 136)].

Amend paragraph beginning at page 183, line 11 of the specification as follows:

Cleavage and fragmentation of the complex by CID afforded information regarding the location of binding of the paromomycin to the chimeric nucleic acid. CID was found to produce no fragmentation at the dA sites in the nucleic acid. Thus paromomycin must bind at or near all three dA residues. Paromomycin therefore is believed to bind to the dA bulge in this RNA/DNA chimeric target, and induces a conformational change that protects all three dA residues from being cleaved during mass spectrometry. See [Figure 41] Figures 41A and 41B.

Amend paragraph beginning at page 184, line 7 of the specification as follows:

The ESI mass spectrum so obtained, shown in [Figure 42] Figures 42A and 42B, demonstrated the presence of new signals for the (M-5H)<sup>5+</sup> ions at m/z values of 1897.8, 1891.3 and 1884.4. Comparing these new signals to the ion peak for the 27-mer alone the observed values of m/z of those members of the combinatorial library that are binding to the target can be calculated. The masses of the binding members of the library were determined to be 566.5, 534.5 and 482.5, respectively. Knowing the structure of the scaffold, and substituents used in the generation of this library, it was possible to determine what substitution pattern (combination of substituents) was present in the binding molecules.

Amend paragraph beginning at page 195, line 22 of the specification as follows:

The QXP method was used to derive an accurate structure of a bound ligand to the RNA target. The NMR structure of the bacterial 16S ribosomal A site bound to paromomycin (Fourmy *et al.*, *Science*, **1996**, 274, 1367; PDB ID: 1pbr) was used as the reference state. The aminoglycoside antibiotic was removed from the ligand-RNA complex. The conformation space of paromomycin was exhaustively searched using the QXP method for the lowest energy conformers. The target RNA was held rigid whereas the paromomycin was treated as fully flexible. Multiple docking searches with the randomly disrupted paromomycin as initial structures were performed. The representative lowest energy structure identified from the search (dark grey) is superimposed on the NMR structure (light grey) of the bound complex [as shown in Figure137. The robustness of the

QXP method is indicated (in Figure 138), through a correlation between the observed rms deviation and QXP energy scores].

Amend paragraph beginning at page 196, line 15 of the specification as follows:

FTMS spectrum was obtained from a mixture of a 16S RNA model (10 mM) and a 60-member combinatorial library. Signals from complexes are highlighted in the insert. Binding of a combinatorial library containing 60 members to the 16S RNA model have been examined under conditions where each library member was present at 5-fold excess over the RNA. As shown in [Figure139] Figure 59, complexes between the 16S RNA and ~5 ligands in the library were observed.

Amend paragraph beginning at page 196, line 21 of the specification as follows:

An expanded view of the 1863 complex from Figure [139] 59 is shown in Figure [140] 60. Two of the compounds in the library had a nominal mass of 398.1 Da. Their calculated molecular weights based on molecular formulas indicate that they differ in mass by 46 mDa. Accurate measurement of the molecular mass for the respective monoisotopic (all  $^{12}\text{C}$ ,  $^{14}\text{N}$ , and  $^{16}\text{O}$ )  $[\text{M}-5\text{H}]^{5-}$  species of the complex ( $m/z$  1863.748) and the free RNA ( $m/z$  1784.126) allowed the mass of the ligand to be calculated as  $398.110 \pm .009$  Da.

Amend paragraph beginning at page 196, line 27 of the specification as follows:

[Figure141] Figure 61 shows high resolution ESI-FTICR spectrum of the library used in Figures [139] 59 and [140] 60, demonstrating that both library members with a nominal molecular weight of 398.1 were present in the synthesized library.

Amend paragraph beginning at page 197, line 3 of the specification as follows:

Based on the high precision mass measurement of the complex, the mass of the binding ligand was determined to be consistent with the library member having a chemical formula of

$C_{15}H_{16}N_4O_2F_6$  and a molecular weight of 398.117 Da (Figure [142] 62). Thus, the identity of the binding ligand was unambiguously established.

Amend paragraph beginning at page 197, line 8 of the specification as follows:

Use of exact mass measurements and elemental constraints can be used to determine the elemental composition of an “unknown” binding ligand. General constraints on the type and number of atoms in an unknown molecule, along with a high precision mass measurement, allow determination of a limited list of molecular formulas which are consistent with the measured mass. Referring to Figure [143] 63, the elemental composition is limited to atoms of C, H, N, and O and further constrained by the elemental composition of a “known” moiety of the molecule. Based on these constraints, the enormous number of atomic combinations which result in a molecular weight of  $615.2969 \pm 0.0006$  are reduced to two possibilities. In addition to unambiguously identifying intended library members, this technique allows one skilled in the art to identify unintended synthetic by-products which bind to the molecular target.

Amend paragraph beginning at page 197, line 20 of the specification as follows:

The results of direct determination of solution phase dissociation constants ( $K_d$ 's) by mass spectrometry is shown in Figure [144] 64. ESI-MS measurements of a solution containing a fixed concentration of RNA at different concentrations of ligand were obtained. By measuring the ratio of bound:unbound RNA at varying ligand concentrations, the  $K_d$  was determined by 1/slope of the “titration curve”. The MS derived value of 110 nM is in good agreement with previously reported literature value of 200 nM.

Amend paragraph beginning at page 197, line 27 of the specification as follows:

[A schematic representation for] For the determination of ligand binding site by tandem mass spectrometry [is shown in Figure 145. A] , a solution containing the molecular target or targets is mixed with a library of ligands and given the opportunity to form noncovalent complexes in solution. These noncovalent complexes are mass analyzed. The noncovalent complexes are

subsequently dissociated in the gas phase via IRMPD or CAD. A comparison of the fragment ions formed from dissociation of the complex with the fragment ions formed from dissociation of the free RNA reveals the ligand binding site.

Amend paragraph beginning at page 198, line 7 of the specification as follows:

Figure [146] 65 shows MASS screening of a 27 member library against a 27-mer RNA construct representing the prokaryotic 16S A-site. The inset reveals that a number of compounds formed complexes with the 16S A-site.

Amend paragraph beginning at page 198, line 11 of the specification as follows:

MS/MS of a 27-mer RNA construct representing the prokaryotic 16S A-site containing deoxyadenosine residues at the paromomycin binding site is shown in Figure [147] 66. The top spectrum was acquired by CAD of the  $[M-5H]5^-$  ion ( $m/z$  1783.6) from uncomplexed RNA and exhibits significant fragmentation at the deoxyadenosine residues. The bottom spectrum was acquired from by CAD of the  $[M-5H]5^-$  ion of the 16S-paromomycin complex ( $m/z$  1907.5) under identical activation energy as employed in the top spectrum. No significant fragment ions are observed in the bottom spectrum consistent with protection of the binding site by the ligand.

Amend paragraph beginning at page 198, line 19 of the specification as follows:

Two combinatorial libraries containing 216 tetraazacyclophanes dissolved in DMSO were mixed with a buffered solution containing 10 mM 16S RNA (see [Figure149] Figure 68) such that each library member was present at 100 nM. The resulting mass spectra, shown in Figure [148] 67 reveal >10 complexes between 16S RNA and library members with the same nominal mass. MS-MS spectra obtained from a mixture of a 27-mer RNA construct representing the prokaryotic 16S A-site containing deoxyadenosine residues at the paromomycin binding and the 216 member combinatorial library. In the top spectrum, ions from the most abundant complex from the first library ( $[M-5H]5^-$ ;  $m/z$  1919.0) were isolated and dissociated. Dissociation of this complex generates three fragment ions at  $m/z$  1006.1, 1065.6, and 1162.4 that result from cleavage at each dA residue. More intense

signals are observed at  $m/z$  2378.9, 2443.1, and 2483.1. These ions correspond to the w21(3-), a20-B(3-), and a21-B(3-) fragments bound to a library member with a mass of  $676.0 \pm 0.6$  Da. The relative abundances of the fragment ions are similar to the pattern observed for uncomplexed RNA, but the masses of the ions from the lower stem and tetraloop are shifted by complexation with the ligand. This ligand offers little protection of the deoxyadenosine residues, and must bind to the lower stem-loop. The library did not inhibit growth of bacteria. In the bottom spectrum, dissociation of the most abundant complex from a mixture of 16S RNA and the second library having  $m/z$  1934.3 with the same collisional energy yields few fragment ions, the predominant signals arising from intact complex and loss of neutral adenine. The reduced level of cleavage and loss of adenine for this complex is consistent with binding of the ligand at the model A site region as does paromomycin. The second library inhibits transcription/translation at 5 mM, and has an MIC of 2-20 mM against *E. coli*(imp-) and *S. pyogenes*.

Amend paragraph beginning at page 199, line 13 of the specification as follows:

Figure [149] 68 shows secondary structures of the 27 base RNA models used in this work corresponding to the 18S (eukaryotic) and 16S (prokaryotic) A-sites. The base sequences differ in seven positions (bold), the net mass difference between the two constructs is only 15.011 Da. Mass tags were covalently added to the 5' terminus of the RNA constructs using tradition phosphoramadite coupling chemistry.

Amend paragraph beginning at page 199, line 18 of the specification as follows:

Methodology to increase the separation between the associated signals in the mass spectra was developed in view of the overlap among signals from RNAs 16S and 18S. RNA targets modified with additional uncharged functional groups conjugated to their 5'-termini were synthesized. Such a synthetic modification is referred to herein as a neutral mass tag. The shift in mass, and concomitant  $m/z$ , of a mass-tagged macromolecule moves the family of signals produced by the tagged RNA into a resolved region of the mass spectrum. ESI-FTICR spectrum of a mixture of 27-base representations of the 16S A-site with (7 mM) and without (1 mM) an 18 atom neutral

mass tag attached to the 5'-terminus in the presence of 500 nM paromomycin is shown in [Figure 150] Figure 69. The ratio between unbound RNA and the RNA-paromomycin complex was equivalent for the 16S and 16S+tag RNA targets demonstrating that the neutral mass tag does not have an appreciable effect on RNA-ligand binding.

Amend paragraph beginning at page 200, line 3 of the specification as follows:

Paromomycin, lividomycin (MW = 761.354 Da), sisomicin (MW = 447.269 Da), tobramycin (MW = 467.2591 Da), and bekanamycin (MW = 483.254 Da) were obtained from Sigma (St. Louis, MO) and ICN (Costa Mesa, CA) and were dissolved to generate 10 mM stock solutions. 2' methoxy analogs of RNA constructs representing the prokaryotic (16S) rRNA and eukaryotic (18S) rRNA A-site (Figure [149] 68) were synthesized in house and precipitated twice from 1 M ammonium acetate following deprotection with ammonia (pH 8.5). The mass-tagged constructs contained an 18-atom mass tag ( $C_{12}H_{25}O_9$ ) attached to the 5'-terminus of the RNA oligomer through a phosphodiester linkage.

Amend paragraph beginning at page 200, line 26 of the specification as follows:

Mass spectrometry experiments were performed in order to detect complex formation between a library containing five aminoglycosides (Sisomicin (Sis), Tobramycin (Tob), Bekanamycin (Bek), Paromomycin (PM), and Lividomycin (LV)) and two RNA targets simultaneously. Signals from the  $(M-5H+)^{5-}$  charge states of free 16S and 18S RNAs are detected at  $m/z$  1801.515 and 1868.338, respectively. As shown in Figure [151] 69, the mass spectrometric assay reproduces the known solution binding properties of aminoglycosides to the 16S A site model and an 18S A site model with a neutral mass linker. Consistent with the higher binding affinity of these aminoglycosides for the 16S A-site relative to the 18S A-site, aminoglycoside complexes are observed only with the 16S rRNA target. Note the absence of 18S-paromomycin and 18S-lividomycin complexes, which would be observed at the  $m/z$ 's indicated by the arrows. The inset demonstrates the isotopic resolution of the complexes. Using multiple isotope peaks of the  $(M-5H+)^{5-}$  and  $(M-4H+)^{4-}$  charge states of the free RNA as internal mass standards, the average mass



measurement error of the complexes is 2.1 ppm. High affinity complexes were detected between the 16S A site 27mer RNA and paromomycin and lividomycin, respectively. Weaker complexes were observed with sisomycin, tobramycin and bekamycin. No complexes were observed between any of the aminoglycosides and the 18S A site model. Thus, this result validates the mass spectrometric assay for identifying compounds that will bind specifically to the target RNAs. No other type of high throughput assay can provide information on the specificity of binding for a compound to two RNA targets simultaneously. The binding of lividomycin to the 16S A site had been inferred from previous biochemical experiments. The mass spectrometer has been used herein to measure a KD of 28 nM for lividomycin and 110 nM for paromomycin to the 16S A site 27mer. The solution KD for paromomycin has been estimated to be between 180 nM and 300 nM.

Amend paragraph beginning at page 202, line 1 of the specification as follows:

The 27-mer model of a segment of the bacterial A site region has been prepared as a full ribonucleotide (see Figure [152] 71, compound R), and as a chimeric 2'-O-methylribonucleotide containing three deoxyadenosine residues (see Figure [152] 71, compound C). RNAs R and C have been prepared using conventional phosphoramidite chemistry on solid support. Phosphoramidites were purchased from Glen Research and used as 0.1 M solutions in acetonitrile. RNA R was prepared following the procedure given in Wincott, *et al.*, *Nucl. Acids Res.*, **1995**, 23, 2677-2684, the disclosure of which is incorporated herein by reference in its entirety. RNA C was prepared using standard coupling cycles, deprotected, and precipitated from 10 M NH<sub>4</sub>OAc. The aminoglycoside paromomycin binds to both R and C with kD values of 0.25 and 0.45 micromolar, respectively. The reported kD values are around 0.2  $\mu$ M. Recht, *et al.*, *J. Mol. Biol.*, **1996**, 262, 421-436, Wong, *et al.*, *Chem. Biol.*, **1998**, 5, 397-406, and Wang, *et al.*, *Biochemistry*, **1997**, 36, 768-779. Paromomycin has been shown previously to bind in the major groove of the 27mer model RNA and induce a conformational change, with contacts to A1408, G1494, and G1491. Miyaguchi, *et al.*, *Nucl. Acids Res.*, **1996**, 24, 3700-3706; Fourmy, *et al.*, *Science*, **1996**, 274, 1367-1371; and Fourmy, *et al.*, *J. Mol. Biol.*, **1998**, 277, 333-345.

Amend paragraph beginning at page 202, line 17 of the specification as follows:

The mass spectrum obtained from a 5  $\mu$ M solution of C mixed with 125 nM paromomycin (Figure [153A] 72A) contains [M-5H]5- ions from free C at m/z 1783.6 and the [M-5H]5- ions of the paromomycin-C complex at m/z 1907.3. Mass spectrometry experiments have been performed on an LCQ quadrupole ion trap mass spectrometer (Finnigan; San Jose, CA) operating in the negative ionization mode. RNA and ligand were dissolved in a 150 mM ammonium acetate buffer at pH 7.0 with isopropyl alcohol added (1:1 v:v) to assist the desolvation process. Parent ions have been isolated with a 1.5 m/z window, and the AC voltage applied to the end caps was increased until about 70% of the parent ion dissociates. The electrospray needle voltage was adjusted to -3.5 kV, and spray was stabilized with a gas pressure of 50 psi (60:40 N<sub>2</sub>:O<sub>2</sub>). The capillary interface was heated to a temperature of 180 °C. The He gas pressure in the ion trap was 1 mTorr. In MS-MS experiments, ions within a 1.5 Da window having the desired m/z were selected via resonance ejection and stored with q ) 0.2. The excitation RF voltage was applied to the end caps for 30 ms and increased manually to 1.1 Vpp to minimize the intensity of the parent ion and to generate the highest abundance of fragment ions. A total of 128 scans were summed over m/z 700-2700 following trapping for 100 ms. Signals from the [M-4H]4- ions of C and the complex are detected at m/z 2229.8 and 2384.4, respectively. No signals are observed from more highly charged ions as observed for samples denatured with tripropylamine. In analogy with studies of native and denatured proteins, this is consistent with a more compact structure for C and the paromomycin complex. The CAD mass spectrum obtained from the [M-5H]5- ion of C is presented in Figure [153B] 72B. Fragment ions are detected at m/z 1005.6 (w6)2-, 1065.8 (a7-B)2-, 1162.6 (w7)2-, 1756.5 (M-Ad)5-, 2108.9 (w21-Ad)3-, 2153.4 (a20-B)3-, 2217.8 (w21)3-, and 2258.3 (a21-B)3-. McLuckey, *et al.*, *J. Am. Soc. Mass Spectrum.*, **1992**, 3, 60-70 and McLuckey, *et al.*, *J. Am. Chem. Soc.*, **1993**, 115, 12085-12095. These fragment ions all result from loss of adenine from the three deoxyadenosine nucleotides, followed by cleavage of the 3'-C-O sugar bonds. The CAD mass spectrum for the [M-5H]5- ion of the complex between C and paromomycin obtained with the same activation energy is shown in Figure [153C] 72C. No fragment ions are detected from strand cleavage at the deoxyadenosine sites using identical dissociation conditions of Figure [153B] 72B. The change in fragmentation pattern

observed upon binding of paromomycin is consistent with a change in the local charge distribution, conformation, or mobility of A1492, A1493, and A1408 that precludes collisional activation and dissociation of the nucleotide.

Amend paragraph beginning at page 203, line 18 of the specification as follows:

Two combinatorial libraries containing 216 tetraazacyclophanes dissolved in DMSO were mixed with a buffered solution containing 10  $\mu$ M C such that each library member is present at 100 nM. The resulting mass spectra reveal >10 complexes between C and library members with the same nominal mass. Ions from the most abundant complex from the first library ( $[M-5H]^{-5}$ ,  $m/z$  1919.0) were isolated and dissociated. As shown in Figure [154A] 73A, dissociation of this complex generates three fragment ions at  $m/z$  1006.1, 1065.6, and 1162.4 that result from cleavage at each dA residue. More intense signals are observed at  $m/z$  2378.9, 2443.1, and 2483.1. These ions correspond to the  $w_{21}^{(3-)}$ ,  $a_{20}-B^{(3-)}$ , and  $a_{21}-B^{(3-)}$  fragments bound to a library member with a mass of 676.0 = 0.6Da. The relative abundances of the fragment ions are similar to the pattern observed for uncomplexed C, but the masses of the ions from the lower stem and tetraloop are shifted by complexation with the ligand. This ligand offers little protection of the deoxyadenosine residues, and must bind to the lower stem-loop. The libraries have been synthesized from a mixture of charged and aromatic functional groups, and are described as libraries 25 and 23 in: An, *et al.*, *Bioorg. Med. Chem. Lett.*, **1998**, in press. Dissociation of the most abundant complex from a mixture of C and the second library having  $m/z$  1934.3 with the same collisional energy (Figure [154B] 73B) yields few fragment ions, the predominant signals arising from intact complex and loss of neutral adenine. The mass of the ligand (753.5 Da) is consistent with six possible compounds in the library having two combinations of functional groups. The reduced level of cleavage and loss of adenine from this complex is consistent with binding of the ligand at the model A site region as does paromomycin. The second library inhibits transcription/translation at 5  $\mu$ m, and has an MIC of 2-20  $\mu$ M against *E. coli* (imp-) and *S. pyogenes*.

Amend paragraph beginning at page 205, line 17 of the specification as follows:

It is preferred that such data collection and database manipulation be achieved through a general purpose digital computer. An exemplary software program has been created and used to identify the small molecules bound to an RNA target, calculate the binding constant, and write the results to a relational database. The program uses as input a file that lists the elemental formulas of the RNA and the small molecules which are present in the mixture under study, and their concentrations in the solution. The program first calculates the expected isotopic peak distribution for the most abundant charge state of each possible complex, then opens the raw FTMS results file. The program performs a fast Fourier transform of the raw data, calibrates the mass axis, and integrates the signals in the resulting spectrum such as the exemplary spectrum shown in Figure [155] 74. The peaks in the spectrum are preferably identified via centroiding as shown in Figure [156] 75, are integrated, and preferably stored in a database. An exemplary data file is shown in Figure [157] 76. The expected and observed peaks are correlated, and the integrals converted into binding constants based on the intensity of an internal standard. The compound identity and binding constant data are written to a relational database. This approach allows large amounts of data that are generated by the mass spectrometer to be analyzed without human intervention, which results in a significant savings in time.

Amend paragraph beginning at page 206, line 3 of the specification as follows:

[Figure155] Figure 74 depicts electrospray ionization Fourier transform ion cyclotron resonance mass spectrometry of a solution which is 5 mM in 16S RNA (Ibis 16628) and 500 nM in the ligand Ibis10019. The raw time-domain dataset is automatically apodized and zero-filled twice prior to Fourier transformation. The spectrum is automatically post-calibrated using multiple isotope peaks of the  $(M-5H+)^{5-}$  and  $(M-4H+)^{4-}$  charge states of the free RNA as internal mass standards and measuring the  $m/z$  difference between the free and bound RNA. The isotope distribution of the free RNA is calculated a priori and the measured distribution is fit to the calculated distribution to ensure that  $m/z$  differences are measured between homoisotopic species (e.g. monoisotopic peaks or isotope peaks containing 4  $^{13}C$  atoms).

Amend paragraph beginning at page 206, line 12 of the specification as follows:

Figure [156] 75 shows isotope clusters observed in the m/z range where RNA-ligand complexes are expected are further analyzed by peak centroiding and integration. Figure [157] 76 depicts data tabulated and stored in a relational database. Peaks which correspond to complexes between the RNA target and ligands are assigned and recorded in the database. If an internal affinity standard is employed, a relative Kd is automatically calculated from the relative abundance of the standard complex and the unknown complex and recorded in the database. Figure [158] 77 depicts a flow chart for one computer program for effectuating certain aspects of the present invention.

**In the Claims:**

Claims 1-86, 101-107 and 109 have been cancelled without prejudice to their presentation in another application.

Claims 87, 88, 94, 95 and 108 have been amended as follows.

87. (Amended) [An] A purified and isolated RNA comprising a joined sequence of at least twenty-nine but not more than seventy nucleotides and having secondary structure defined by:

- five nucleotides forming a first side of a first double stranded region;
- four nucleotides forming a first side of a first end loop region;
- five nucleotides forming a second side of said first double stranded region;
- two nucleotides forming a bulge between said first double stranded region and a second double stranded region;
- five nucleotides forming a first side of [a]said second double stranded region;
- three nucleotides forming a second end loop region; and
- five nucleotides forming a second side of said second double stranded region.

88. (Amended) The RNA of claim 87 wherein said nucleotides forming said first side of said first double stranded region are of the sequence NNNGA, UAAGA, AAAGA, UAUGA, or UUUGA and said nucleotides forming said second side of said first doubled stranded region are of the sequence [GNGNN, GGGCU, or GCGUG] UUNNG, UUUUG, or UUCUG.

94. (Amended) A purified and isolated RNA comprising a joined sequence of nucleotides having secondary structure defined by:

five nucleotides forming a first side of a first double stranded region;  
four nucleotides forming a first side of a first end loop region;  
five nucleotides forming a second side of said first double stranded region;  
two nucleotides forming a bulge between said first double stranded region and a second double stranded region;  
five nucleotides forming a first side of [a] said second double stranded region;  
three nucleotides forming a second end loop region; and  
five nucleotides forming a second side of said second double stranded region.

95. (Amended) The RNA of claim 94 wherein said nucleotides forming said first side of said first double stranded region are of the sequence NNNGA, UAAGA, AAAGA, UAUGA, or UUUGA and said nucleotides forming said second side of said first double stranded region are of the sequence [GNGNN, GGGCU, or GCGUG] UUNNG, UUUUG, or UUCUG.

108. (Amended twice) [An] A purified and isolated RNA comprising the consensus sequence NNNGAUNCUUUNNGUAAGCCCNANGNGNN (SEQ ID NO:23) and having a first double stranded region, a first end loop region, a second double stranded region, and a second end loop region.